Cerebral Cortex, April 2020;30: 2167–2184

doi: 10.1093/cercor/bhz230
Advance Access Publication Date: 11 November 2019
Original Article

ORIGINAL ARTICLE

Lack of Sez6 Family Proteins Impairs Motor Functions, Short-Term Memory, and Cognitive Flexibility and Alters Dendritic Spine Properties

Amelia Nash[1], Timothy D. Aumann[2], Martina Pigoni[3], Stefan F. Lichtenthaler[3,4,5], Hiroshi Takeshima[6], Kathryn M. Munro[1] and Jenny M. Gunnersen[1,2]

[1]Department of Anatomy and Neuroscience, University of Melbourne, Melbourne, VIC 3010, Australia, [2]The Florey Institute of Neuroscience and Mental Health, University of Melbourne, Melbourne, VIC 3010, Australia, [3]German Centre for Neurodegenerative Diseases (DZNE), Munich 81377, Germany, [4]Neuroproteomics, School of Medicine, Klinikum rechts der Isar, and Institute for Advanced Study, Technical University of Munich, Munich 81675, Germany, [5]Munich Cluster for Systems Neurology (SyNergy), Munich 81377, Germany, and [6]Division of Pharmaceutical Sciences, Graduate School and Faculty of Pharmaceutical Sciences, Kyoto University, Kyoto 606-8501, Japan

Address correspondence to Jenny M. Gunnersen. Email: jenny.gunnersen@unimelb.edu.au
Kathryn M. Munro and Jenny M. Gunnersen are equal senior authors

Abstract

Seizure-related gene 6 (Sez6), Sez6-Like (Sez6L), and Sez6-Like 2 (Sez6L2) comprise a family of homologous proteins widely expressed throughout the brain that have been linked to neurodevelopmental and psychiatric disorders. Here, we use Sez6 triple knockout (TKO) mice, which lack all three Sez6 family proteins, to demonstrate that Sez6 family proteins regulate dendritic spine structure and cognitive functions, motor learning, and maintenance of motor functions across the lifespan. Compared to WT controls, we found that Sez6 TKO mice had impaired motor learning and their motor coordination was negatively affected from 6 weeks old and declined more rapidly as they aged. Sez6 TKO mice had reduced spine density in the hippocampus and dendritic spines were shifted to more immature morphologies in the somatosensory cortex. Cognitive testing revealed that they had enhanced stress responsiveness, impaired working, and spatial short-term memory but intact spatial long-term memory in the Morris water maze albeit accompanied by a reversal deficit. Our study demonstrates that the lack of Sez6 family proteins results in phenotypes commonly associated with neuropsychiatric disorders making it likely that Sez6 family proteins contribute to the complex etiologies of these disorders.

Key words: behavior, cortex, neuron, hippocampus

Introduction

Neurodevelopmental and psychiatric disorders are complex, multimodal, and frequently multigenic disorders that can involve circuit wide dysfunction. The genetic basis of many of these disorders is not fully understood, however common to these disorders is the dysregulation of genes involved in synaptic function and communication (O'Dushlaine et al. 2011; Nurnberger et al. 2014; De Rubeis et al. 2014; Hormozdiari et al. 2015; Wang et al. 2018). The seizure-related gene 6 (Sez6) family of proteins plays a role in synaptic development and

function (Miyazaki et al. 2006; Gunnersen et al. 2007), and genetic variants in human homologs of Sez6 family proteins have been linked to neurodevelopmental and psychiatric disorders including autism spectrum disorder (ASD; Kumar et al. 2008; Weiss et al. 2008; Konyukh et al. 2011; Cukier et al. 2014; Chapman et al. 2015; Mariani et al. 2015), intellectual disability (Gilissen et al. 2014), childhood onset schizophrenia (Ambalavanan et al. 2016), and bipolar disorder (Xu et al. 2013). To better understand how aberrant functioning of Sez6 proteins may contribute to the etiology of these conditions, it is crucial we identify the physiological roles of the Sez6 family members and whether disruptions mimic the synaptopathies characteristic of neurodevelopmental and psychiatric disorders.

All three Sez6 family members, Sez6, Sez6-Like (Sez6L), and Sez6-Like 2 (Sez6L2), are expressed widely throughout the brain including in the cortex, hippocampus, striatum, and cerebellum (Miyazaki et al. 2006; Gunnersen et al. 2007; Osaki et al. 2011). Sez6 family proteins are transmembrane proteins, which contain CUB (complement subcomponent C1r, C1s/sea urchin embryonic growth factor Uegf/bone morphogenetic protein1) and SCR (short consensus repeat) domains in their extracellular regions (Shimizu-Nishikawa et al. 1995; Gunnersen et al. 2007). These interaction domains are commonly found in proteins of the complement system but are also present in some central nervous system (CNS) proteins (Morley and Campbell 1984; Bork and Beckmann 1993; Sia et al. 2013; Steen et al. 2013). For example, CUB domain-containing transmembrane proteins NETO1 and NETO2 act as auxiliary proteins for kainate and NMDA neurotransmitter receptors in mice (Ng et al. 2009; Zhang et al. 2009; Copits et al. 2011). In *Caenorhabditis elegans*, SCR domain containing LEV-9 and CUB domain containing LEV-10 cluster acetylcholine receptors at the neuromuscular junction (Gendrel et al. 2009) and CUB domain containing SOL-1 and SOL-2 regulate AMPA receptor functions (Zheng et al. 2004; Wang et al. 2012). Sez6 family proteins also contain an intracellular NPxY internalization motif, which is recognized by accessory clathrin adaptor proteins for endocytosis to clathrin-coated vesicles (reviewed by Pandey 2009). In addition to these motifs, which suggest Sez6 family proteins are involved in binding other extracellular or cell surface proteins, Sez6 family proteins are cleaved close to their transmembrane domains to release their extracellular domain in a process referred to as ectodomain shedding. This shedding is mediated primarily by the Alzheimer's disease (AD) protease β-site amyloid precursor protein cleaving enzyme 1 (BACE1) in the case of Sez6 and Sez6L (Kuhn et al. 2012; Pigoni et al. 2016), and while Sez6L2 may be shed by BACE1 (Kuhn et al. 2012), it is also cleaved by additional proteases, such as Cathepsin D (Boonen et al. 2016). Furthermore, Sez6 subsequently undergoes regulated intramembrane proteolysis by γ-secretase within the transmembrane domain (Pigoni et al. 2016). The shed, soluble form of Sez6, is secreted from neurons (Pigoni et al. 2016) and has been found to be increased in the cerebrospinal fluid (CSF) of patients with depression, bipolar disorder, and schizophrenia (Maccarrone et al. 2013) and inflammatory pain (Roitman et al. 2019).

Of the Sez6 proteins, the expression and role of Sez6 are best characterized, during both development and in the adult brain (Gunnersen et al. 2007) and are known to be required for normal neuronal development and function. Analysis of a constitutive Sez6 knockout (KO) mouse line demonstrated a regulatory role of the Sez6 protein in dendritic branching and dendritic spine density in the cortex (Gunnersen et al. 2007). Altered electrophysiological properties, including reduced postsynaptic responses of cortical neurons in the Sez6 KO brain, were observed along with a memory deficit in the Morris water maze (MWM) probe trial and a motor deficit on the rotarod in Sez6 KO mice (Gunnersen et al. 2007). Constitutive Sez6 KO mice have also been shown to have impaired hippocampal long-term potentiation (LTP; Zhu et al. 2016). Recent results obtained with our conditional Sez6 KO model, in which Sez6 was deleted in a small population of Thy1 expressing neurons, have indicated that the Sez6 protein is important for dendritic spine dynamics not only during development but also in adulthood (Zhu et al. 2016). Less is known about the functions of Sez6L and Sez6L2 in the CNS. Sez6L2 acts as a transport receptor for Cathepsin D and the Cathepsin D-processed form was shown to regulate neurite outgrowth in a neuroblastoma cell line (Boonen et al. 2016). Furthermore, anti-Sez6L2 antibodies have been identified in patients with cerebellar ataxia (Yaguchi et al. 2014; Borsche et al. 2019).

The role of Sez6 family proteins in the cerebellum has been investigated using a triple knockout (TKO) mouse line, which lacks all three Sez6 family members (Miyazaki et al. 2006). It was found that Sez6 family proteins contribute to the refinement of synaptic connectivity between climbing fibers and Purkinje cells (PCs) in the cerebellum. This was demonstrated by the failure of Sez6 TKO neurons to achieve a mature state of mono-innervation of PCs by climbing fibers. Additionally, lack of all Sez6 family proteins resulted in motor deficits, as seen on the rotarod and fixed beam (Miyazaki et al. 2006).

To investigate whether Sez6 family proteins may contribute to phenotypes observed in the neurodevelopmental and psychiatric disorders to which they have been linked, we probed a variety of cognitive processes governed by the forebrain by performing a comprehensive battery of behavioral tests on Sez6 TKO mice and analysis of neuron morphology using the Golgi-Cox technique. The role of Sez6 family members in learning and memory was of particular interest, given the widespread expression of Sez6 family members across the forebrain and strong expression in the hippocampus (Gunnersen et al. 2007; Osaki et al. 2011; Pigoni et al. 2016). We show here that Sez6 family proteins are required for motor learning as well as a range of motor functions and determine that the combined lack of Sez6 family proteins biases dendritic spines on somatosensory cortical neurons toward immature morphologies and decreases spine density on CA1 hippocampal neurons. The global lack of Sez6 family proteins further impacts on emotional and cognitive domains with Sez6 TKO mice exhibiting enhanced fear learning and stress responsiveness, impaired working memory, and cognitive inflexibility in the MWM task.

Materials and Methods

Animals

For behavioral testing and dendritic spine analysis, mice with targeted deletions of the genes encoding Sez6, Sez6L, and Sez6L2 (Sez6 TKO) and control wild-type (WT) mice were maintained on a mixed 129 and C57BL6 genetic background. The Sez6 TKO mouse line was kindly provided by Professor Hiroshi Takeshima (Miyazaki et al. 2006). All mice were housed in the Biomedical Sciences Animal Facility, University of Melbourne and were group housed unless otherwise noted. Mice were given food and water ad libitum during housing and lights were on between 7 AM and 7 PM. All animal experiments were approved by the Animal Ethics Committee at the University of Melbourne.

DAB Immunostaining

Brains from 4% paraformaldehyde perfusion-fixed WT ($n = 3$) and Sez6 TKO ($n = 3$) adult mice (4–5 months old) were cryosectioned (14 µm) and underwent sequential incubation in Bloxall (Vector Laboratories), 5% Bovine Serum Albumin (BSA; Sigma Aldrich) and 0.3% Triton X-100 (Sigma Aldrich) in phosphate buffered saline (PBS), and avidin/biotin (Avidin/Biotin Blocking Kit, Vector Laboratories). Sections were incubated overnight with monoclonal rat anti-Sez6 (1:100), monoclonal rat anti-Sez6L (1: 100; both kindly provided by M.P.), or polyclonal sheep anti-Sez6L2 (1:1000; R&D Systems) antibodies diluted in 5% BSA and 0.1% Triton X-100. Sections were washed with PBS, incubated with biotinylated goat anti-rat IgG (1: 750; Vector Laboratories) or rabbit anti-sheep IgG (1: 750; Vector Laboratories), and processed using the Vectastain ABC Kit (Vector Laboratories) and ImmPACT DAB peroxidase substrate (Vector Laboratories) according to manufacturer's instructions. Primary or secondary antibodies were omitted on sections of each experiment to confirm staining specificity. Images were acquired at ×4 or ×10 magnification on an Olympus BX61 microscope using cellSens software (Olympus Corporation).

Golgi-Cox Impregnation

Modified Golgi-Cox impregnation of neurons was performed using the FD RapidGolgi Stain kit (FD NeuroTechnologies Inc.). Brains from 2- to 3-month-old behaviorally naïve male mice (WT, $n = 6$; TKO, $n = 6$) were fixed, sectioned at 100 µm, and developed in parallel. For dendritic analysis, the basal dendritic branches (within the 100 µm section) of 30 layer V somatosensory cortex pyramidal neurons per genotype were traced with Neurolucida software (MBF Bioscience). Two secondary basal dendritic segments (20–45 µm in length) from each of these neurons were then analyzed for dendritic spine properties as described by Risher et al. (2014). Spines with a head width >0.5 µm (rather than 0.6 µm) were classed as mushroom spines. Z-stack brightfield images were captured on an Olympus BX61 microscope (Olympus Corporation) using analySIS software (Soft Imaging System GmbH). For spine analysis in the hippocampus (WT, $n = 7$; TKO, $n = 7$), approximately 20 µm lengths of oblique secondary dendrite from neurons in the stratum radiatum of CA1 pyramidal neurons were selected. Z-stack images were captured using brightfield on a Zeiss Axio Imager M2 (Zeiss) using Stereo Investigator (MBF Bioscience).

Behavioral Testing

All behavioral tests were performed in the light cycle and a total of 8 age-matched cohorts of mice were used. Cohort 1 male mice underwent rotarod testing. Cohort 2 male mice underwent repeated testing on the inverted screen test, fixed beam, grip strength, and ledge beam at 6, 12, 24, and 46 to 48 weeks of age. Cohort 3 singly housed male and group-housed female mice were tested in the MWM. Cohort 4 male and female mice were tested on the elevated open field (EOF). Cohort 5 male mice underwent multiple tests spaced over a month in the following order: elevated zero maze, novel arm Y maze, social interaction, and Digigait. Cohort 6 male mice were tested in the locomotor cell. Cohort 7 female mice were tested on the Digigait and then in context fear conditioning (CFC). Cohort 8 male and female mice underwent multiple tests over 1 month in the following order: Digigait, CFC, spontaneous alternation, and novel object recognition (NOR).

Rotarod

Two- to 3-month-old male mice (WT, $n = 17$; TKO, $n = 16$) were tested on the accelerating rotarod (IITC Life Science Inc.). Mice underwent 3 trials per day over 4 days with each trial lasting 5 mins and an intertrial interval of at least 10 min. The rods were 9.5 cm in diameter and accelerated from 1 to 23 rotations per minute (RPM) over the 5-min trial.

Locomotor Cell

Three- to 4-month-old male mice (WT, $n = 8$; TKO, $n = 8$) were tested for locomotor activity under low lighting conditions (10 lux). Mice were placed in the center of the locomotor cell (27.5 cm × 27.5 cm × 13.5 cm; Med Associates Inc.), and locomotor activity in the horizontal and vertical planes was recorded over a 30-min period.

Longitudinal Motor Testing

Male mice underwent repeated testing in the fixed beam, ledge beam, and grip strength tests at 6, 12, 24, and 46 to 48 weeks of age as described below.

Fixed Beam

Mice (WT, $n = 10$; TKO, $n = 8$) were placed onto a stainless steel beam 60 cm long and either 20 mm or 26 mm in diameter, suspended 40 cm above a padded surface, and secured to an escape point at one end. Immediately before testing, mice undertook 3 training traversals on the 26 mm beam at increasing distances from the escape point. During testing, mice were placed at the unsecured end of the beam and the time taken to traverse the beam was recorded. Mice were tested first on the 26 mm beam then on the 20 mm beam.

Ledge Beam

Mice (WT, $n = 10$; TKO, $n = 8$) were placed onto an 80 cm long Perspex beam that narrowed from 3.5 cm to 1 mm along its length. About 1 cm below this beam on either side was a 0.5-cm wide ledge that the mice could use to recover if their feet slipped from the beam. Mice performed 3 days of training with 3 traversals per day prior to testing. On the test day, mice traversed the beam once while being recorded. Videos of the left and right sides were analyzed for foot faults, and data were recorded as faults per step where steps were the total number of hind paw placements made.

Grip Strength

To measure grip strength, mice (WT, $n = 20$; TKO, $n = 17$) were placed with their forepaws gripping the bar of the apparatus (Ametek) and were pulled steadily backward by the tail until their grip released. Mice had 5 attempts separated by 30 s, and the maximum force exerted by the mice was recorded. Grip strength was calculated by dividing this maximum force value by the weight of the mouse.

Digigait

Male and female mice approximately 3 months old (WT, $n = 33$, TKO, $n = 26$) underwent gait analysis using the DigiGait Imaging System (Mouse Specifics Inc.). Mice ran on a transparent treadmill (15 cm × 5 cm) at a speed of 25 cm/s and 4 s of video

was acquired for analysis. Parameters analyzed: stance width, the distance between either the two forepaws or two hindpaws; stride length, the distance between consecutive strides measured from the same paw; stride frequency, steps per second; stride time, sum of stance and swing durations; stance duration, paw contact with treadmill; swing duration, no paw contact with treadmill; propulsion phase, maximal paw contact with treadmill to just before swing phase; and brake duration, initial to maximal paw contact with treadmill.

Elevated Open Field

Male and female mice (WT, $n = 16$; TKO, $n = 16$) approximately 3 months old were tested on the EOF, a test arena (75 cm × 100 cm) without walls situated 60 cm above the ground. Overhead lighting was switched off and two spotlights on either side of the EOF shone directly onto the field to create an aversive environment. Mice were placed in the center of the field and allowed to roam freely for 3 min. Videos were obtained and analyzed using TopScan Lite (CleverySys Inc.). Time moved was recorded by the investigator.

Zero Maze

Male and female mice (WT, $n = 20$; TKO, $n = 20$) 3–4 months old were tested in the zero maze, a modification of the elevated plus maze without the ambiguous center zone. The zero maze was elevated 60 cm above the ground and consisted of two walled quadrants and two open quadrants. Overhead lighting was switched off and two dim uplights were placed ~1 m behind each of the walled quadrants. Mice were placed into one of the two walled quadrants (alternated between mice) to start and allowed to roam freely for 5 min. Videos were obtained and analyzed using TopScan Lite (CleverSys Inc.).

CFC and Extinction

Male and female mice approximately 3 months old (WT, $n = 24$; TKO, $n = 24$) were used for tests of fear conditioning and subsequent extinction. The fear conditioning chamber was a 25 cm × 30 cm × 24 cm plexiglass chamber (CleverSys Inc.) equipped with a stainless steel shock grid floor. Visual cues on the chamber walls and a light cue were used. In the training session, mice were allowed to explore the chamber for 180 s before receiving 3× 0.8 mA shocks of 2 s with 30 s between each shock. Mice remained in the chamber for an additional 60 s before being removed to their home cage. Freezing time was measured for the 180 s pre-shock and for the 60 s immediately post shock. A test was performed 24 h after the initial fear conditioning and extinction sessions occurred daily thereafter for a further 6 days. In these test and extinction sessions, mice were placed back into the chamber and allowed to explore freely for 180 s without receiving a shock. Fear behavior (percentage time freezing) was recorded and analyzed by FreezeScan software (CleverSys Inc.).

Y Maze Spontaneous Alternation

Male and female mice (WT, $n = 27$; TKO, $n = 26$) underwent Y maze spontaneous alternation testing. The Y maze had 3 equally spaced arms of dimensions 30 cm × 11 cm × 18 cm. Arms were labeled as A, B, or C and the starting arm was rotated between mice. Arm entries were scored over a 10-min trial. The starting arm position was not counted as an entry; entries were only counted once all four paws had crossed into the arm. Overhead lighting was switched off and 3 dim uplights placed around the room were on for testing. Videos were captured and distance traveled was analyzed using TopScan Lite software (CleverSys Inc., USA). Arm entry order was recorded by the investigator and spontaneous alternation percentage was calculated as: number of spontaneous alternations/(total number of arm entries—2) × 100 (Miedel et al. 2017).

Novel Arm Y Maze

Three–month-old male mice (WT, $n = 10$; TKO, $n = 10$) underwent Y maze spatial memory testing. Mice were placed in the home arm at the start of each trial. In the training trial, one arm was sectioned off by a removable divider and the mice were allowed to explore the two available arms for 10 min. After a 2-h interval, each mouse underwent a 5-min test trial where they were able to explore all arms, including the previously inaccessible "novel" arm. Overhead lighting was switched off and 3 dim uplights placed around the room were on for training and testing. Videos were obtained and analyzed using TopScan Lite software (CleverSys Inc.). The amount of time spent in the novel arm was compared to the averaged time spent in the 2 familiar arms.

Novel Object Recognition

Male and female mice 3–4 months old were used for NOR testing. Mice had a 5-min habituation session in the empty chamber (40 cm × 40 cm) immediately prior to the testing period. During the sample phase, mice were placed in the chamber and allowed to investigate 2 identical objects for 5 min. Mice were removed from the chamber for 2 h and one object was replaced with a novel object before the mice were placed back into the chamber and allowed to explore for a further 2 min for the test phase. The object set used in the sample phase and the side the novel object appeared on during the test phase were alternated between mice. Time spent investigating each object during the test phase was recorded and analyzed using TopScan Lite software (CleverSys Inc.) where investigation was defined as the nose being within ~1 cm of the object. Mice were unable to climb onto either of the object sets used.

Morris Water Maze

Singly housed male mice and group-housed female mice approximately 3 months old (WT, $n = 18$; TKO, $n = 16$) were used for the MWM. Each mouse underwent 4 trials per day, starting at 1 of 4 locations equally spaced around the pool (1.2 m diameter). Prominent geometric images and 3D spatial cues were arrayed around the room and the investigator was hidden from sight during testing. Overhead lighting was switched off and a bright uplight was placed on top of one of the 3D spatial cues. The 10-cm diameter platform was submerged 1 cm under the surface of the water, which was made opaque with white, nontoxic paint. Each trial lasted a maximum of 120 s, and at the end of each trial, the mouse was either placed or allowed to stay on the platform for 20 s. The location of the platform was kept constant for the 7 consecutive days of acquisition testing. An automated tracking system (TopScan Lite, CleverySys Inc.) recorded and analyzed swim paths. The day after acquisition training was completed, the probe trial took place. For the probe trial, the platform was removed and each mouse was placed into the pool once starting from the location directly opposite where

the hidden platform had been located. The 30-s probe trial was analyzed to determine whether mice had learnt the task. Immediately after the probe trial was completed, all mice began reversal training. For reversal training, the hidden platform was moved to a different quadrant and the platform location was kept constant for 4 consecutive days. Reversal trials were conducted as described for initial acquisition testing. The day after the reversal training finished, each mouse completed a 30-s probe trial. Mouse search strategy categorization was performed as described by Brody and Holtzman (2006), and trials were then grouped into either spatial or nonspatial categories for analysis.

Electrophysiology

Prefrontal cortex slices (300 µm thick) were prepared from ~4-week-old WT and Sez6 TKO male mice. Mice were anesthetized with isoflurane before they were killed by decapitation. Coronal slices were cut with a vibratome (Integraslice, Campden Instruments) from the whole forebrain in an ice-cold (0 °C) dissecting solution (125 mM NaCl, 25 mM $NaHCO_3$, 3 mM KCl, 1.25 mM $NaH_2PO_4{\cdot}H_2$, 1 mM $CaCl_2$, 6 mM $MgCl_2$, 25 mM glucose, bubbled with 95% O_2 and 5% CO_2, pH 7.4) then transferred to 37 °C artificial CSF (ACSF, 125 mM NaCl, 25 mM $NaHCO_3$, 3 mM KCl, 1.25 mM $NaH_2PO_4{\cdot}H_2$, 2 mM $CaCl_2$, 1 mM $MgCl_2$, 2 mM glucose, bubbled with 95% O_2 and 5% CO_2, pH 7.4). Slices were allowed to recover for at least 45 min before being transferred into a bath perfused with ASCF at 32 °C for recording. Layer V pyramidal neurons in the prefrontal cortex were selected for recording based on morphological characteristics. Whole-cell recordings were made from single neurons using glass micropipettes (~1 µm tip diameter, ~6–10 MΩ resistance) containing internal solution (135 mM K-Gluconate, 7 mM NaCl, 10 mM HEPES, 2 mM $MgCl_2$, 2 mM Na_2-ATP, pH 7.2). For all recordings, neurons were held at −70 mV and a range of electrophysiological properties were measured in current-clamp and single-electrode voltage-clamp mode using an Axoclamp 2B amplifier (3 kHz bandwidth) and Clampex 9.0 software. Recordings were digitized to disc at 10 kHz using an Axon Digidata 1550. All electrophysiological analyses were performed in Clampfit 10 software (Molecular Devices, LLC) with steady-state current measured approximately 47 ms from the onset of the voltage step. Spontaneous excitatory postsynaptic potential files were additionally bandpass filtered with highpass cutoff set to 10 Hz and lowpass cutoff to 1000 Hz.

Statistical Analysis

Supplementary Table 1 indicates the statistical test used for each experiment, *n*, *P*, and *F*/*t* values as well as degrees of freedom. Where appropriate, data were tested for normality using D'Agostino–Pearson omnibus normality test. As indicated by Box's test of equality of covariance matrices, data were transformed with a $\log_{10}$ transformation for pathlength and latency MWM data or a square root transformation for platform crossings MWM data. If Mauchly's test of sphericity was determined to be significant, the Greenhouse-Geisser correction was used. The Bonferroni post hoc test was used for all relevant analyses. All data are represented as mean ± standard error of the mean (SEM), except for the MWM probe trials which are represented as mean ± 95% confidence interval (CI; as per Rogers et al. 2017). Results were considered statistically significant when a $P < 0.05$ was obtained. Data were analyzed in GraphPad Prism 7 (GraphPad Software Inc.), IBM SPSS Statistics 25 (IBM Corporation), or Minitab 18 (Minitab Inc.).

Results

Sez6 Family Proteins Are Expressed Widely Throughout the Brain

mRNA in situ hybridization has previously been used to look at expression of all three Sez6 family members in the adult brain (Miyazaki et al. 2006), and protein expression of Sez6 and Sez6L in the adult brain has been investigated using immunohistochemistry (Gunnersen et al. 2007; Osaki et al. 2011; Pigoni et al. 2016). To investigate Sez6 family protein expression throughout the entire brain, we used DAB immunohistochemistry on sagittal and coronal sections of WT brains (Fig. 1 and Supplementary Fig. 1, respectively). Specificity of the Sez6 and Sez6L antibodies we used has been confirmed previously (Pigoni et al. 2016), and we confirmed specificity of the Sez6L2 antibody by staining sagittal Sez6 TKO sections (Supplementary Fig. 2). Consistent with previous reports (Gunnersen et al. 2007; Osaki et al. 2011; Pigoni et al. 2016), we saw Sez6 protein expression in layers V and VI of the cortex (Supplementary Fig. 1*A*), CA1 region of the hippocampus (Supplementary Fig. 1*D*), striatum and olfactory bulb with weak expression apparent for the rest of the brain (Fig. 1*A*), and cerebellum (Supplementary Fig. 1*G*). Again, Sez6L protein staining was consistent with mRNA in situ hybridization and previous immunohistochemistry (Miyazaki et al. 2006; Pigoni et al. 2016). In contrast to Sez6, Sez6L protein expression was widespread throughout the brain (Fig. 1*B*) including the cortex, with strongest expression in layers II/III and layer V (Supplementary Fig. 1*B*), and all regions of the hippocampus (Supplementary Fig. 1*E*), although staining was more concentrated in the processes rather than the cell body. There was also significant staining of the olfactory bulb, striatum, thalamus, hypothalamus, midbrain, and cerebellum, with staining of PC bodies and processes readily apparent (Supplementary Fig. 1*H*). Similar to Sez6L protein expression, staining of Sez6L2 revealed widespread expression throughout the brain (Fig. 1*C*). Staining for Sez6L2 protein was present in the cortex with staining of cell bodies in layers II/III to VI (Supplementary Fig. 1*C*) and in all regions of the hippocampus where, similar to Sez6, staining was concentrated in the cell body. Sez6L2 staining was also apparent in the olfactory bulb, striatum, thalamus, hypothalamus, midbrain, and cerebellum with strong staining of Sez6L2 in the cell bodies and processes of PCs (Supplementary Fig. 1*I*).

Lack of All Sez6 Family Proteins Results in a Motor Deficit that Worsens with Age

Sez6 TKO mice were found to display a motor deficit on the fixed speed rotarod and the fixed beam, associated with aberrant refinement of climbing fiber to PC connectivity in the cerebellum (Miyazaki et al. 2006), but a detailed analysis of motor and behavioral deficits is lacking. To further explore the role of Sez6 proteins in motor learning and function, we tested Sez6 TKO and WT mice on an accelerating rotarod over consecutive days. Consistent with the observation of Miyazaki et al. (2006), the Sez6 TKO mice showed a significant impairment on the rotarod compared to WT mice with a shorter latency to fall at every trial (Fig. 2*A*; 2-way repeated measures (RM) ANOVA genotype × trial $F_{11, 341} = 11.2$, interaction $^{****}P < 0.0001$). Furthermore, Sez6 TKO mice were slower to learn the task; their latency to fall did not significantly increase until trial 9 (Bonferroni post hoc test TKO trial 1 vs. trial 9, $^{***}P = 0.0002$), whereas WT mice showed improvement by trial 2 (WT trial 1 vs. trial 2, $^{****}P < 0.0001$).

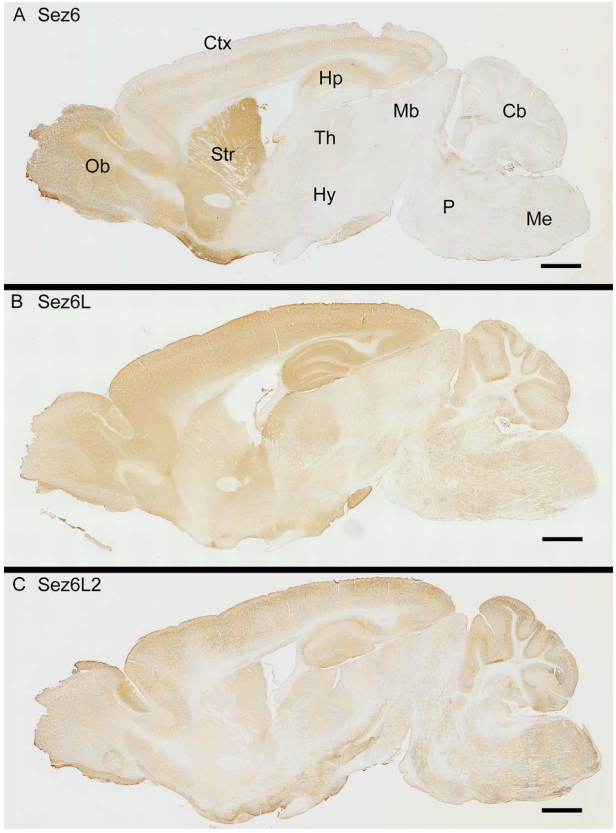

Figure 1. Sez6 family protein expression in the adult mouse brain demonstrates widespread expression of Sez6L and Sez6L2 but a more restricted pattern for Sez6. (*A*) A high level of Sez6-immunoreactivity (IR) was observed in the olfactory bulb, striatum, lower layers of the cortex, and CA1 region of the hippocampus. (*B*) A high level of Sez6L-IR was observed throughout the brain including the olfactory bulb, striatum, cortex, hippocampus, and cerebellum. (*C*) A high level of Sez6L2-IR was observed throughout the brain including the olfactory bulb, striatum, cortex, hippocampus, and cerebellum. Cb, cerebellum; Ctx, cerebral cortex; Hp, hippocampus; Hy, hypothalamus; Mb, midbrain; Me, medulla; Ob, olfactory bulb; P, pons; Str, striatum; Th, thalamus. Scale bar 1 mm.

Next, we assessed general locomotor activity under non-stressful conditions by testing WT and Sez6 TKO mice in locomotor cells. Sez6 TKO mice displayed a general locomotor deficit over the 30-min testing period, moving a significantly shorter distance than WT mice (Fig. 2B; WT: 8009 cm ± 803, TKO: 3890 cm ± 569, unpaired *t* test $^{***}P = 0.0009$). Additionally, Sez6 TKO mice reared significantly less than WT mice over the testing period (Fig. 2C; TKO: 114 ± 26, WT: 256 ± 27 vertical counts, unpaired *t* test $^{**}P = 0.0018$).

To determine the effect of age on the Sez6 TKO motor impairment, mice underwent longitudinal testing for certain motor tasks. Mice were first tested at 6 weeks of age and subsequently tested at 12, 24, and 46–48 weeks of age. On the fixed beam, Sez6 TKO mice were slower to traverse beams of both diameters than WT mice at all ages (Fig. 2D, 20 mm beam 2-way RM ANOVA genotype × age interaction $F_{1.97, 31.5} = 34$, $^{****}P < 0.0001$; Fig. 2E, 26 mm beam two-way RM ANOVA genotype x age interaction $F_{1.78, 28.5} = 22.3$, $^{****}P < 0.0001$). Post hoc within genotype comparisons revealed that WT animals were able to improve their performance on both beams from 6 to 12 weeks (20 mm beam 6 weeks: 4.2 s ± 0.3, 12 weeks: 3.1 s ± 0.2, Bonferroni post hoc $^{*}P = 0.013$; 26 mm beam 6 weeks: 4.2 s ± 0.2, 12 weeks: 2.8 s ± 0.1, Bonferroni post hoc $^{**}P = 0.002$), and this performance did not diminish with age (Fig. 2D, 20 mm 6 weeks vs. 48 weeks, Bonferroni post hoc $P > 0.99$; Fig. 2E, 26 mm 6 weeks vs. 48 weeks, Bonferroni post hoc $P > 0.99$). On the other hand, TKO mice did show age-related decline in performance. While they also improved their performance from 6 to 12 weeks, by 24 weeks of age they were traversing the narrower 20 mm beam more slowly than at 6 weeks of age (Fig. 2D; 6 weeks: 7.2 s ± 0.4, 24 weeks: 9.2 s ± 0.5, Bonferroni post hoc $^{*}P = 0.02$) and by 48 weeks they were traversing both beams significantly more slowly than at 6 weeks of age (Fig. 2D, 20 mm beam 6 weeks: 7.2 s ± 0.4, 48 weeks: 14.1 s ± 0.97, Bonferroni post hoc $^{****}P < 0.0001$; Fig. 2E, 26 mm beam 6 weeks: 6.3 s ± 0.5, 48 weeks: 10.02 s ± 0.9, Bonferroni post hoc $^{***}P = 0.001$).

Ledge beam testing, where mice must traverse a beam that becomes progressively narrower along its length, demonstrated that Sez6 TKO mice made significantly more forepaw faults than WT mice at 24 and 48 weeks of age (Fig. 2F; 2-way RM ANOVA genotype $F_{1, 16} = 8.39$, $^{*}P = 0.011$; age $F_{3, 48} = 0.429$, $P = 0.733$; interaction $F_{3, 48} = 1.98$, $P = 0.13$) and significantly more hind-paw faults than WT mice at all time-points tested (Fig. 2G; two-way RM ANOVA genotype $F_{1, 16} = 70.4$, $^{****}P < 0.0001$; age $F_{3, 48} = 3.25$, $^{*}P = 0.03$; interaction $F_{3, 48} = 2.54$, $P = 0.067$). Additionally, as Sez6 TKO mice aged their hind-paw performance on the ledge beam deteriorated (6 weeks: 0.38 faults/step ±0.042, 48 weeks: 0.54 faults/step ±0.031, Bonferroni post hoc $^{*}P = 0.044$), while WT mice maintained their performance over time (6 weeks: 0.19 faults/step ±0.038, 48 weeks: 0.19 faults/step ±0.028, Bonferroni post hoc P = ns). The increased foot faults made by Sez6 TKO mice on the ledge beam were not due to increased beam traversal speed as they traversed the ledge beam significantly slower than WT mice at all ages tested (Supplementary Fig. 3).

Testing with a grip strength meter to assess forelimb muscle strength revealed that WT mice were able to exert a slightly, but significantly greater force with their forelimbs than Sez6 TKO mice at 6, 12, and 24 weeks of age (Fig. 2H; 2-way RM ANOVA genotype × age interaction $F_{3, 105} = 2.52$, $^{***}P = 0.0004$). It was only at 48 weeks of age that Sez6 TKO mice were able to exert equivalent force (WT: 2.78 ± 0.21; TKO: 2.99 ± 0.15; Bonferroni post hoc P = ns).

Digigait, which measures multiple parameters of the mouse gait, was used to gain a greater understanding of why the Sez6 TKO animals were performing poorly in motor tests, particularly on the fixed and ledge beams and rotarod. Mice ran on a treadmill at a speed of 25 cm/s and gait was analyzed and compared between genotypes. Digigait analysis revealed that the stance width distance between both forepaws and hindpaws was significantly wider in Sez6 TKO mice compared to WT mice (Fig. 2I; forepaws, WT: 1.63 cm ± 0.03, TKO: 1.8 cm ± 0.04; unpaired *t* test $^{**}P = 0.0035$; hindpaws, WT: 2.41 cm ± 0.04, TKO: 2.83 cm ± 0.04; unpaired *t* test $^{****}P < 0.0001$). Sez6 TKO mice also displayed a number of related gait alternations (Supplementary Table 2). Stride length was increased in Sez6 TKO mice, and this was accompanied by a decrease in stride frequency. Although the overall duration of the Sez6 TKO stride was not significantly different from WT, breakdown of stride parameters revealed that both the stance and swing phase of the stride were significantly longer in Sez6 TKO mice. Furthermore, braking time of the stance portion of the stride was significantly reduced while

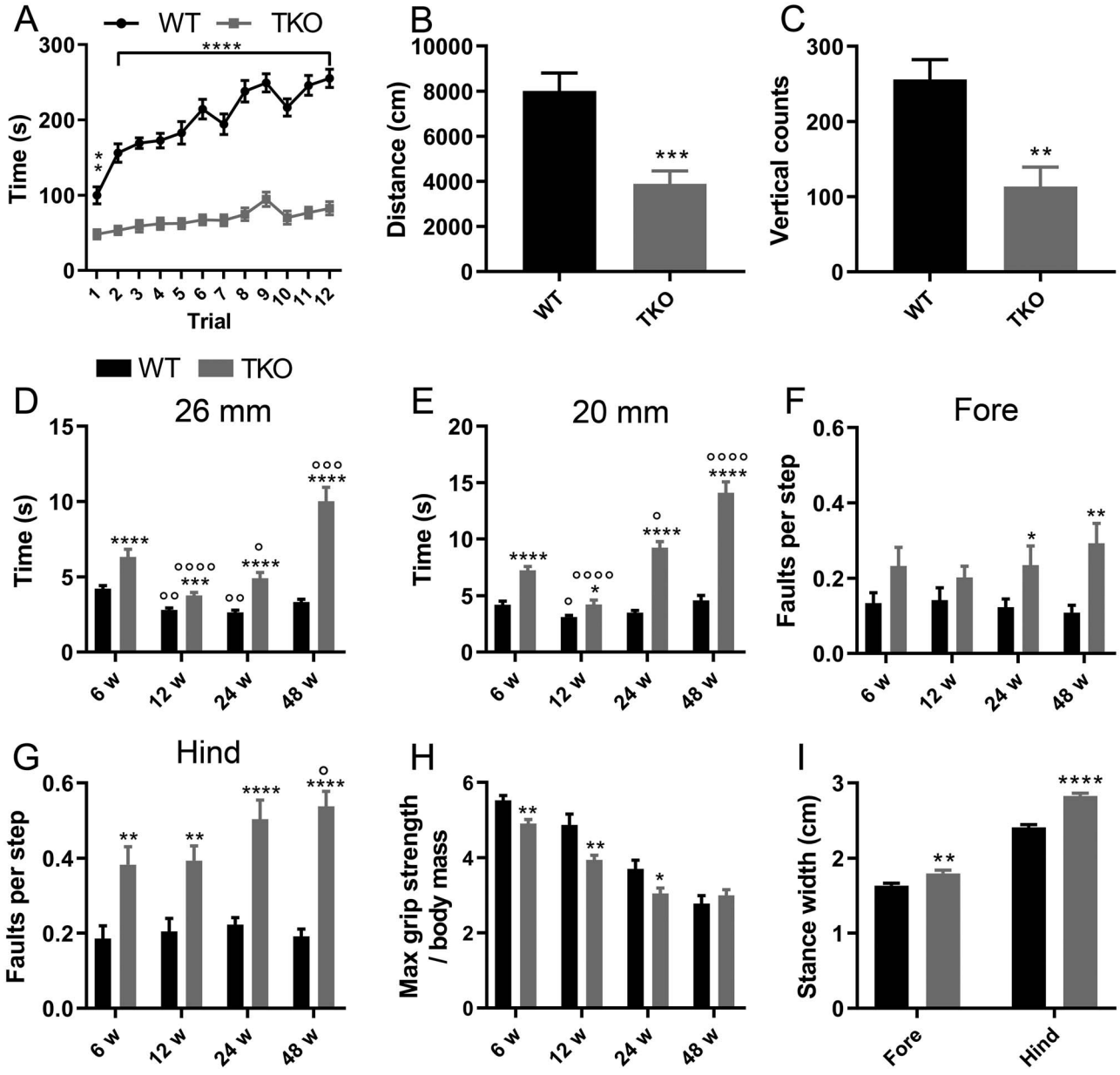

Figure 2. Sez6 family KO mice display motor deficits. (*A*) Accelerating rotarod performance is impaired in Sez6 TKO mice ($n = 16$) compared with WT ($n = 17$). (*B*) Locomotor activity of Sez6 TKO mice ($n = 8$) over a 30-min test is reduced compared to WT ($n = 8$) in the locomotor cell. (*C*) Rearing behavior (represented as vertical counts) is reduced in Sez6 TKO mice in the locomotor cell. (*D*, *E*) Sez6 TKO mice ($n = 8$) took longer to traverse fixed beams of diameters 20 mm (*D*) and 26 mm (*E*) than WT mice ($n = 10$). (*F*, *G*) Performance on the ledge beam apparatus is impaired in Sez6 TKO mice ($n = 8$) compared to WT mice ($n = 10$). Faults per step made by forelimb (*F*) and hindlimb (*G*) on the ledge beam. (*H*) Grip strength of forelimbs was weaker in Sez6 TKO mice ($n = 17$) compared to WT ($n = 20$) at three of four time points tested. (*I*) Gait analysis of Sez6 TKO ($n = 26$) and WT ($n = 33$) mice at 25 cm/s. Sez6 TKO mice had a wider stance while running of both the forelimbs and hindlimbs. Data were compared using a 2-way RM analysis of variance (ANOVA) (*A*, *D*–*H*) or an unpaired *t* test (*B*, *C*, and *I*). All data are represented as mean ± SEM. Between genotype comparison: $^{*}P < 0.05$, $^{**}P < 0.01$, $^{***}P < 0.001$, $^{****}P < 0.0001$; within genotype comparison to 6 weeks of age: $^{\circ}P < 0.05$, $^{\circ\circ}P < 0.01$, $^{\circ\circ\circ}P < 0.001$, $^{\circ\circ\circ\circ}P < 0.0001$. w, week; fore, forelimb; hind, hindlimb.

the propulsion phase was significantly increased in Sez6 TKO mice.

Lack of Sez6 Family Proteins Alters Dendritic Spine Morphology and Number

Previously, we identified a role for the Sez6 protein in regulating dendritic growth and patterning in the developing cortex (Gunnersen et al. 2007). To determine the impact of gene deletion of all three Sez6 family members on dendrite length and number, basal dendritic trees of somatosensory layer V pyramidal neurons were traced in sections from Golgi-Cox impregnated brains. Both the number and length of basal dendritic branches were unchanged in TKO mice compared with WT mice (Supplementary Fig. 4). Previous studies have also demonstrated a role for the Sez6 protein in maintaining dendritic spine density (Gunnersen et al. 2007; Zhu et al. 2016). To examine whether the decrease in dendritic spine density

was exacerbated when all three Sez6 family members were absent, spines of secondary basal dendrites were counted and classified. Overall, spine density was found to be the same in WT and Sez6 TKO somatosensory layer V pyramidal neurons (Fig. 3A; nested $F_{1, 10.4} = 0.37$, ANOVA $P = 0.556$); however, Sez6 TKO neurons were found to have a lower density of mushroom (Fig. 3B; WT: 0.42 ± 0.02 spines/µm; TKO: 0.28 ± 0.016 spines/µm, nested ANOVA $F_{1, 10.1} = 16.1$, $^{**}P = 0.002$) and branched spines (WT: 0.068 spines/µm ± 0.0066; TKO: 0.042 spines/µm ± 0.0058, nested ANOVA $F_{1, 100} = 8.11$, $^{**}P = 0.005$) than controls and a higher density of thin and stubby spines (thin spines WT: 0.29 spines/µm ± 0.02; TKO: 0.4 spines/µm ± 0.026, nested ANOVA $F_{1, 9.9} = 5.16$, $^{*}P = 0.047$ and stubby spines WT: 0.057 spines/µm ± 0.007; TKO: 0.17 spines/µm ± 0.016, nested ANOVA $F_{1, 10.6} = 10$, $^{**}P = 0.009$). This shift away from mature spine types in the Sez6 TKO cortex was accompanied by a decrease in both the average length and average width of spines compared to WT (Fig. 3C; spine length WT: 1.1 µm ± 0.023; TKO: 0.86 µm ± 0.036, nested ANOVA $F_{1, 10.5} = 5.83$, $^{*}P = 0.035$ and spine width WT: 0.58 µm ± 0.0073; TKO: 0.50 µm ± 0.0079, nested ANOVA $F_{1, 10.2} = 22$, $^{***}P = 0.001$). However, the ratio between spine length and head width was the same in Sez6 TKO mice compared to WT (Fig. 3D; nested ANOVA $F_{1, 10.5} = 0.84$, P = ns).

Dendritic spine morphology and density were also scored on oblique dendrites of pyramidal neurons in the CA1 stratum radiatum layer of the hippocampus. Alterations in dendritic spine morphology and density in the CA1 region have been linked to memory impairments and intellectual disability (Penzes et al. 2011; Herms and Dorostkar 2016). Hippocampal spine density was slightly but significantly decreased in Sez6 TKO neurons compared to WT (Fig. 3A; WT: 1.74 ± 0.041 spines/µm; TKO: 1.60 ± 0.035 spines/µm, nested ANOVA $F_{1, 49.8} = 5.36$, $^{*}P = 0.025$). Dendritic spine morphology was not significantly changed although there was a trend toward a decreased density of mushroom spines in the Sez6 TKO animals (Fig. 3E; WT: 0.9 ± 0.045; TKO: 0.77 ± 0.034, nested ANOVA $F_{1, 11.35} = 3.83$, $P = 0.076$). Length and width of spines were unchanged between WT and Sez6 TKO animals (Fig. 3C; nested ANOVA: length $F_{1, 44.3} = 2.95$, P = ns; width $F_{1, 12.3} = 0.12$, P = ns), as was the length/width ratio (Fig. 3D; nested ANOVA $F_{1, 43.4} = 1.38$, P = ns).

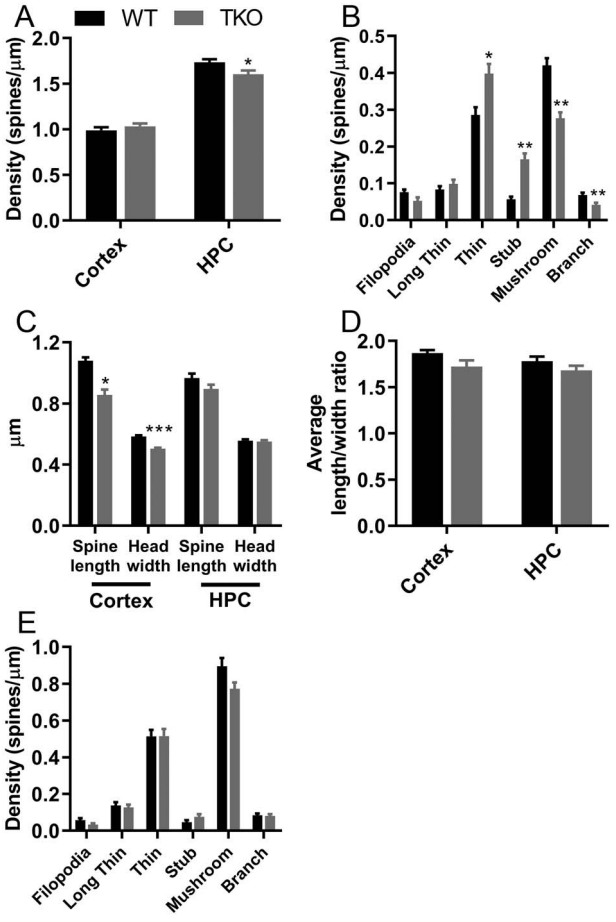

Figure 3. Dendritic spine morphology and density are affected by lack of Sez6 family proteins. (*A*) Density of dendritic spines was unchanged in the somatosensory cortex of Sez6 TKO mice ($n = 6$ mice) compared with WT ($n = 6$ mice) and was reduced in the CA1 region of the hippocampus of Sez6 TKO mice ($n = 7$ mice) compared to WT ($n = 7$ mice). (*B*) Quantification of dendritic spine subtype composition revealed a shift in spine subtype distribution in the somatosensory cortex. (*C*) Length and width of dendritic spines were reduced in the cortex of Sez6 TKO mice compared to WT but were unchanged in the hippocampus. (*D*) The length/width ratio was unchanged between WT and Sez6 TKO mice in both the cortex and hippocampus. (*E*) Quantification of dendritic spine subtype composition revealed no difference between WT and Sez6 TKO in the CA1 region of the hippocampus. All data are represented as mean ± SEM and were analyzed using a nested ANOVA. $^{*}P < 0.05$, $^{**}P < 0.01$, $^{***}P < 0.001$. HPC, hippocampus.

Sez6 TKO Mice Exhibit Altered Anxiety-Related Behavior and Fear Memory

In order to investigate anxiety-related behavior, mice were tested on the EOF, a modification of the open field arena, and the zero maze. The bright lights and large open field with no walls create an aversive environment that has been shown to induce anxiety like behavior in mice (Murphy et al. 2004). During EOF testing, Sez6 TKO mice spent significantly less time moving than WT mice (Fig. 4A; WT: 71.4 s ± 2.56, TKO: 38.7 s ± 5.83; unpaired *t* test $^{****}P < 0.0001$). Sez6 TKO also took longer to leave the center of the open field (Fig. 4B; WT latency: 4.52 s ± 0.67, TKO latency: 12.6 s ± 2.28; unpaired *t* test $^{****}P < 0.001$). Both results indicate that Sez6 TKO mice are more anxious than WT mice in this paradigm. Increased stress responsiveness of Sez6 TKO was further supported by observations on the zero maze. Although Sez6 TKO mice did not spend significantly less time in the open quadrants than WT mice (Fig. 4C; WT 28.9 s ± 2.9, TKO 23.4 s ± 4.8; $P = 0.326$, unpaired *t* test), they made significantly fewer entries to the open quadrants (Fig. 4D; WT 8.9 entries ±1.02; TKO 5.7 entries ±0.96; $^{*}P = 0.0096$, unpaired *t* test) and took longer to leave the starting quadrant (Supplementary Fig. 5A; WT 27.1 s ± 11.1, TKO 88.9 s ± 24.5; $^{*}P = 0.0103$, Mann–Whitney test). Additionally, Sez6 TKO mice had a significantly longer latency to visit the nonstart closed arm (Supplementary Fig. 5B; WT 51.7 s ± 12.4, TKO 224 s ± 23.4; $^{****}P < 0.0001$, Mann–Whitney test) with 45% Sez6 TKO mice never visiting this arm in contrast to 100% of WT mice.

To assess learning and memory in Sez6 TKO mice, mice were analyzed using CFC. The CFC paradigm assesses the degree to which an animal is able to learn to associate a neutral stimulus (the fear conditioning chamber) with an aversive stimulus (the foot shock). One day after training in CFC, mice are placed back into the chamber and their level of freezing, a strong indicator of fear-related behavior, is observed. Furthermore, extinction testing was conducted to determine the ability of the mice to extinguish the association between the neutral and aversive stimuli. Our results indicate that Sez6 TKO mice

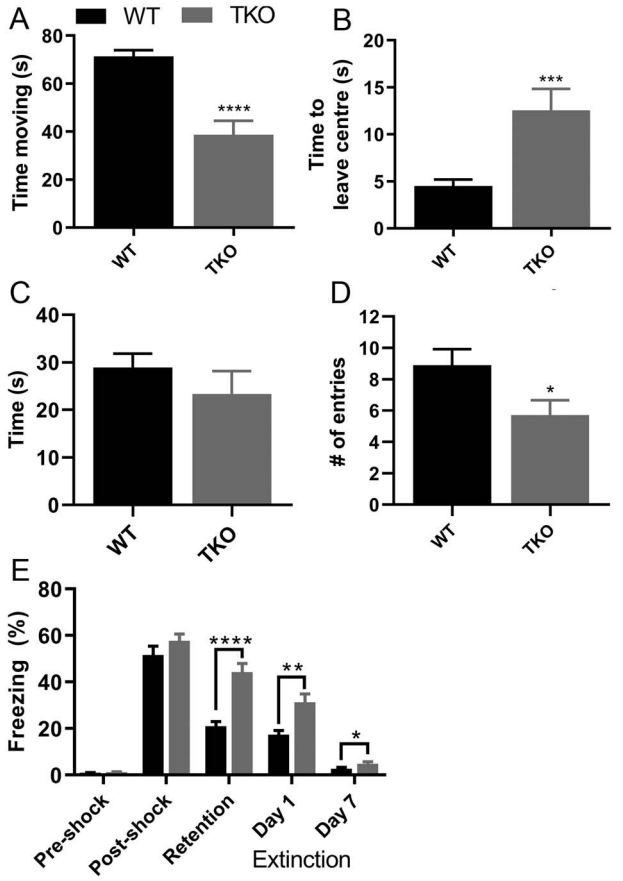

Figure 4. Sez6 family KO mice display enhanced stress responsiveness and fear learning. (*A*, *B*) Performance on the EOF. (*A*) Sez6 TKO mice ($n = 16$) spend less time moving on the EOF compared to WT ($n = 16$). (*B*) Sez6 TKO mice take longer to leave the center of the EOF than WT mice. (*C*, *D*) Sez6 TKO mice are more stress responsive on the zero maze. (*C*) Time spent in the open quadrants of the zero maze is similar between WT ($n = 20$) and TKO ($n = 20$) mice. (*D*) Sez6 TKO mice make significantly less entries in the open quadrants of the zero maze than WT mice. (*E*) Sez6 TKO mice ($n = 24$) display enhanced fear learning and delayed fear extinction as indicted by increased freezing levels compared to WT ($n = 24$). All data are expressed as mean ± SEM and were compared using an unpaired *t* test (*A*, *C*, and *D*), Mann–Whitney test (*B*) or a two-way RM ANOVA (*E*). $^{*}P < 0.05$, $^{**}P < 0.01$, $^{***}P < 0.001$, $^{****}P < 0.0001$.

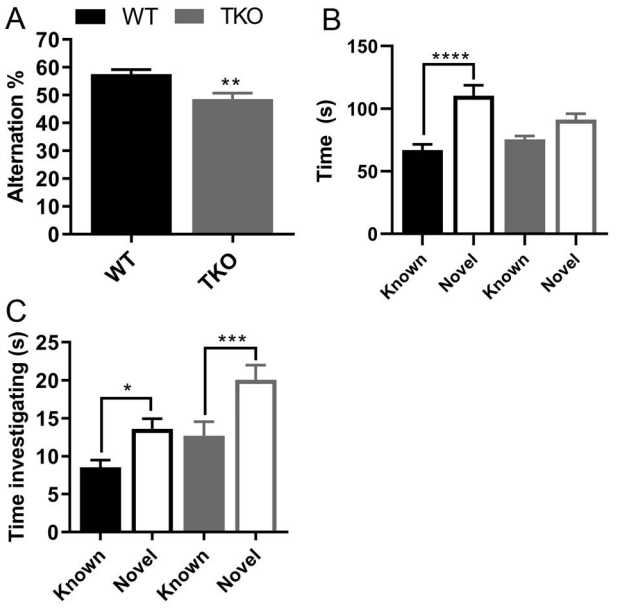

Figure 5. Sez6 family KO mice have impaired working memory and short-term spatial memory but intact short-term object recognition memory. (*A*) Performance in Y maze spontaneous alternation indicates that Sez6 TKO mice ($n = 26$) have impaired spatial working memory compared to WT mice ($n = 27$). (*B*) WT mice ($n = 10$) but not Sez6 TKO mice ($n = 10$) show preference for the novel arm indicating Sez6 TKO mice have impaired spatial short-term memory. (*C*) Both WT ($n = 17$) and Sez6 TKO mice ($n = 17$) preferred to investigate a novel object over a known object. All data expressed as mean ± SEM and were compared using an unpaired *t* test (*A*) or a mixed effects ANOVA (*B*, *C*). $^{*}P < 0.05$, $^{**}P < 0.01$, $^{***}P < 0.001$, $^{****}P < 0.0001$.

acquire the fear memory more strongly than WT mice as they froze significantly more than WTs in the 24-h retention test (Fig. 4E; two-way RM ANOVA genotype × day interaction $F_{2.77,\ 124.8} = 9.92$, $^{***}P = 0.0001$; Bonferroni post hoc retention: WT freezing 20.9% ± 2.07, TKO freezing 44.2% ± 3.78, $^{****}P < 0.0001$). Fear extinction was also found to be delayed in Sez6 TKO mice (Extinction day 1 WT vs. TKO: Bonferroni post hoc $^{***}P = 0.0011$) such that by the final day of extinction, Sez6 TKO mice still displayed significantly more freezing behavior than WT mice (Bonferroni post hoc extinction day 9 WT freezing 2.7% ± 0.6, TKO freezing 4.86% ± 0.83, $^{*}P = 0.04$). Post hoc comparison within genotypes revealed that both genotypes had significantly reduced their freezing response over the extinction period (WT extinction day 1 17.3% ± 1.82, WT extinction day 9 2.7% ± 0.6, $^{****}P < 0.0001$; TKO extinction day 1 31.2% ± 3.6, TKO extinction day 7 4.86% ± 0.83, $^{****}P < 0.0001$) but while WT freezing levels on the final day of extinction were not significantly different from their initial pre-shock freezing levels (WT pre-shock 0.97% ± 0.14, WT extinction day 9 2.7% ± 0.6, $P = 0.197$), Sez6 TKO mice were still freezing significantly more than at pre-shock testing (TKO pre-shock 1.21% ± 0.18, TKO extinction day 9 4.86% ± 0.83, $^{****}P < 0.0001$).

Sez6 TKO Mice Have Deficits in Working Memory, Spatial Short-Term Memory, and Reversal Learning

To investigate working memory in Sez6 TKO, mice were tested by assessing spontaneous alternation in a Y maze. Mice should show a tendency to enter the less recently entered arm and thus need to be able to recall which arms they have previously entered. The spontaneous alternation percentage was significantly different between WT and Sez6 TKO mice (Fig. 5A; WT: 57.6% ± 1.63, TKO: 48.6% ± 2.06; $^{**}P = 0.0013$, unpaired *t* test). Sez6 TKO mice showed significantly fewer arm entries than WT mice (Supplementary Fig. 6A; WT: 45.4 ± 1.84, TKO: 32.9 ± 2.28; $^{****}P < 0.0001$, unpaired *t* test) and traveled significantly less distance (Supplementary Fig. 6B; WT: 2208 cm ± 62.3, TKO: 1527 cm ± 77.4; $^{****}P < 0.0001$, unpaired *t* test); however, there was no significant correlation of alternation percentage with either number of arm entries (Supplementary Fig. 6C; WT $r = -0.2$, $P = 0.32$; TKO $r = -0.048$, $P = 0.82$; Pearson's correlation) or to distance traveled (Supplementary Fig. 6D; WT $r = -0.1$, $P = 0.583$; TKO $r = -0.06$, $P = 0.774$) indicating that these factors did not confound the spontaneous alternation results.

To assess short-term spatial memory, modified Y maze with extra-maze visual cues was used. During the training trial, one arm was blocked from entry. After a 2-h interval, each mouse was placed back in the Y maze with the previously blocked, third "novel" arm now available for entry. A preference for spending

time in the novel arm indicates that a memory of the two previously explored arms has been formed. WT mice showed a clear preference for spending time in the novel arm (Fig. 5B; mixed effects ANOVA: genotype × arm interaction $F_{1, 36} = 6.33$, $^{*}P = 0.0165$; Bonferroni post hoc test: WT novel 110 s ± 8.41, WT known 67 s ± 4.38, $^{****}P < 0.0001$); however, there was no significant difference in the time that Sez6 TKO mice spent in the novel arm compared to the known arm (TKO novel 91.2 s ± 4.84, TKO known 67 s ± 2.67, $P = 0.305$) indicating that Sez6 TKO mice had impaired short-term spatial memory. The short-term memory deficit in the Sez6 TKO mice was restricted to hippocampal-dependent, spatial memory as intact novelty-seeking behavior and short-term memory was observed during NOR testing with both WT and Sez6 TKO mice spending significantly more time investigating the novel object than the familiar object (Fig. 5C; mixed effects ANOVA: genotype $F_{1, 32} = 7.61$, $^{**}P = 0.01$; object $F_{1, 32} = 31.8$, $^{****}P < 0.0001$; interaction $F_{1, 32} = 1.08$, P = ns, Bonferroni post hoc WT known vs. novel $^{*}P = 0.0162$, TKO known vs. novel $^{***}P = 0.0003$).

Given that working memory and short-term spatial memory were impaired, we wanted to further probe spatial long-term memory to achieve a more in-depth understanding of spatial learning and memory in the Sez6 TKO mice. To do this, mice were tested in the MWM with reversal. Over the acquisition phase, Sez6 TKO mice learnt the task as well as WT mice (Fig. 6A,B; 2-way RM ANOVA latency: genotype × day interaction $F_{6, 192} = 3.51$, $^{**}P = 0.0026$; pathlength: genotype × day interaction $F_{6, 192} = 3.34$, $^{**}P = 0.0038$; Bonferroni post hoc revealed no difference in pathlength on day 7: $P = 0.417$) despite having a slower average swim speed (Fig. 6C; two-way RM ANOVA genotype $F_{1, 32} = 72.4$, $^{****}P < 0.0001$, day $F_{4.11, 132} = 2.69$, $^{*}P = 0.032$, interaction $F_{4.11, 132} = 0.911$, P = ns). The slower swim speed is likely the reason Sez6 TKO had a longer latency than WT but an equivalent pathlength on the final training days (Fig. 6A,B). The probe trial demonstrated that both genotypes had acquired the spatial memory at the end of acquisition learning phase (Fig. 6D; 95% CI did not overlap with chance WT: 14.01 s, 95% CI [11.59, 16.43], TKO: 13.67 s 95% CI [9.77, 17.58]).

Mice subsequently underwent reversal learning, which revealed that Sez6 TKO mice had difficulty switching their search strategy in response to a new goal. Sez6 TKO mice had a significantly longer pathlength to the hidden platform than WT across the reversal phase (Fig. 6B; 2-way RM ANOVA genotype $F_{1, 32} = 12.4$, $^{**}P = 0.001$; day $F_{3, 96} = 49.6$, $^{****}P < 0.0001$; interaction $F_{3, 96} = 0.406$, P = ns) and this, along with their slower swim speed, resulted in them taking a longer time to find the platform (Fig. 6A; 2-way RM ANOVA genotype $F_{1, 32} = 60.2$, $^{****}P < 0.0001$; day $F_{3, 96} = 48.1$, $^{****}P < 0.0001$; $F_{3, 96} = 0.869$, interaction P = ns). Sez6 TKO mice demonstrated perseverative behavior, crossing the old platform location more frequently than WT mice on the first and second days of reversal (Fig. 6E; 2-way RM ANOVA genotype $F_{1, 32} = 6.36$, $^{*}P = 0.016$; day $F_{2.82, 73.3} = 74.3$, $^{****}P < 0.0001$; interaction $F_{2.82, 73.3} = 1.46$, P = ns). Categorization of the search strategies used by the mice to find the platform indicated that Sez6 TKO and WT had a similar learning trajectory during the acquisition phase, with both genotypes increasing their use of spatial search strategies from day 1 to day 7 (Fig. 6F, WT day 1 6%, WT day 7 67%, $^{****}P < 0.0001$; Fig. 6G, TKO day 1 12%, TKO day 7 81%, $^{****}P < 0.0001$; Fisher's exact test). By the final day of acquisition learning, both genotypes were using spatial search strategies to a comparable degree (WT day 7 spatial: 66.7%, TKO day 7 spatial: 81.3%; Fisher's exact test $P = 0.079$). In the reversal phase, while WT mice quickly adjusted their search strategy to the new goal location, Sez6 TKO mice used random rather than spatial strategies (WT day 8 spatial 35%, TKO day 8 spatial 8%, Fisher's exact test $^{**}P < 0.001$). Sez6 TKO mice were still using significantly less spatial search strategies than WT mice on the last day of reversal (WT day 11 spatial 81.9%, TKO day 11 spatial 53.1%; Fisher's exact test $^{***}P = 0.0004$). Furthermore, in the reversal probe trial, Sez6 TKO mice failed to show a preference for the target quadrant (Fig. 6D; TKO: 10.88 s, 95% CI [7.47; 14.3]; WT: 14.48 s, 95% CI [12.1, 16.9]) indicating that they had not been able to effectively learn the new platform location.

Sez6 TKO Prefrontal Cortex Neurons Have Altered Spontaneous Postsynaptic Current Properties

Given that many of the behavioral deficits we found in Sez6 TKO mice could be linked to the prefrontal cortex, we investigated potential functional changes in layer V pyramidal neurons from prefrontal cortex. We examined intrinsic neuronal properties and spontaneous excitatory synaptic properties and found that overall the majority of these properties were unchanged in Sez6 TKO mice (see Supplementary Table 3). However, we did find that membrane resistance was lower in Sez6 TKO neurons than in WT neurons (TKO 115.4 MΩ ± 19.4, WT 194.3 MΩ ± 29.2, $^{**}P = 0.0087$, Mann–Whitney test) and that at more positive holding potentials, Sez6 TKO neurons exhibited significantly larger steady-state currents (Supplementary Fig. 7; mixed effects ANOVA: genotype × voltage step interaction $F_{14, 744} = 4.61$, $^{****}P < 0.0001$). Additionally we found that the amplitude of spontaneous excitatory postsynaptic currents in Sez6 TKO neurons was significantly larger than that of WT neurons (TKO 21.1 pA ± 1.36, WT 17.5 pA ± 1.09, $^{*}P = 0.0136$, Mann–Whitney test).

Discussion

In this study, we demonstrate important roles for Sez6 family proteins in the mouse brain through phenotypic characterization of a mouse lacking all three family members (Sez6 TKO). This was particularly important as the overlapping spatial and temporal patterns of expression of Sez6 family proteins in the brain (Miyazaki et al. 2006; Pigoni et al. 2016) indicate the possibility of functional compensation in a single or double KO animal. We show that Sez6 TKO results in a motor impairment that is present from 6 weeks of age and involves changes to both forelimb and hindlimb function and motor learning deficits. Lack of Sez6 family proteins results in a shift to more immature spine phenotypes in the somatosensory cortex and a decreased spine density in the hippocampus. Furthermore, Sez6 TKO mice display an anxiety-like phenotype, enhanced fear memory, working and short-term spatial memory deficits, and cognitive inflexibility.

It has previously been shown that Sez6 family members are involved in motor function as mice lacking all Sez6 family members perform poorly on the fixed speed rotarod and fixed beam (Miyazaki et al. 2006). Our findings complement and expand on this work by revealing that motor dysfunction in Sez6 TKO mice begins in the juvenile period and includes weak forelimb grip and gait alterations that are exacerbated with age. A contributing factor is likely to be the failure of maturation of cerebellar neuronal connectivity reported by Miyazaki et al. (2006), who demonstrated that PCs in adult Sez6 TKO mice aberrantly retained innervation from multiple climbing fibers

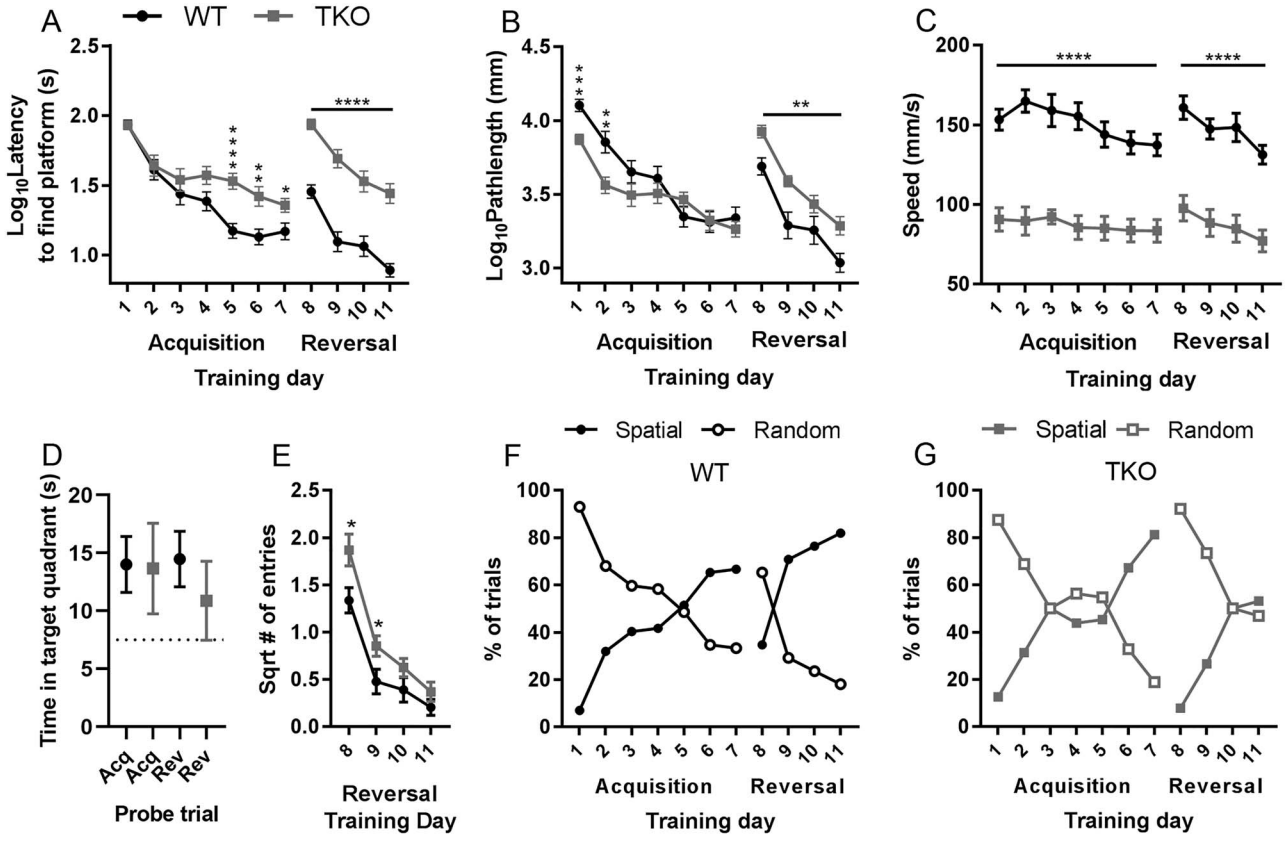

Figure 6. Performance in the MWM is negatively affected by lack of Sez6 family proteins. Sez6 TKO mice ($n = 16$) learn the hidden platform location just as well as WT ($n = 18$) during the acquisition phase but have difficulty learning the new platform location during the reversal phase. (*A*) Sez6 TKO mice were slower than WT to find the platform during the last few days of acquisition and were significantly slower at finding the hidden platform during the reversal phase. (*B*) Sez6 TKO mice were more efficient at finding the hidden platform location on the first 2 days of the acquisition phase but swam significantly further than WT mice on day 8 of the reversal phase. (*C*) During both the acquisition and reversal training, Sez6 TKO mice had a slower average swim speed than WT mice. (*D*) Probe trials revealed both WT and Sez6 TKO mice had successfully learnt the hidden platform location during the acquisition phase, as 95% CI did not overlap with chance (7.5 s), but only WT mice successfully learnt the reversal location. (*E*) Sez6 TKO mice made more entries to the old platform location on the first 2 days of the reversal phase. (*F*, *G*) Search strategy use by WT (*F*) and Sez6 TKO (*G*) mice across the acquisition and reversal phases. WT and TKO mice used spatial strategies equally as often on the last day of acquisition training but Sez6 TKO mice were using significantly less spatial search strategies on day 11 of reversal compared with WT. Data are expressed as mean ± SEM (*A*–*C*, *E*), mean ± 95% CI (*D*) or as percentage of trials using a given search strategy as a function of genotype and day of hidden platform testing (*F*, *G*). Data were analyzed by two-way RM ANOVA (*A*–*C*, *E*) or Fisher's exact test (*F*, *G*). $^{*}P < 0.05$, $^{**}P < 0.01$, $^{***}P < 0.001$, $^{****}P < 0.0001$. acq, acquisition; rev, reversal.

(CFs). This synaptic phenotype has been observed to accompany motor dysfunction in mice (Crépel et al., 1980; Chen et al., 1995; Kano et al., 1997; Kakizawa et al., 2000). People with ASD often display motor dysfunction, including motor coordination difficulties that implicate the cerebellum and basal ganglia (Barbeau et al. 2015; reviewed by Paquet et al. 2016). The patDp/+ mouse model of the human 15q11–13 duplication syndrome associated with ASD not only demonstrates gait abnormalities closely resembling those of the Sez6 TKO mouse but also retains multiinnervation of PCs by CFs and demonstrates a motor learning impairment (Piochon et al. 2014). It is important to note that expression of Sez6 family proteins, while high in the developing and adult cerebellum, is also strong in other regions of the CNS important for motor coordination and motor learning, namely the motor cortex, striatum, and spinal cord (Lein et al. 2007; Osaki et al. 2011; Allen Institute for Brain Science). The striatum, for example, plays a key role in motor learning, with rotarod performance decreased upon disruption of striatal function (Dang et al. 2006; Yin et al. 2009; Durieux et al. 2012), while the spinal cord has a well-documented role in generating and regulating gait (reviewed by Kiehn 2016). We cannot rule out a contribution of these additional motor areas to the phenotype we observed in Sez6 TKO mice; in fact the early failure of synaptic refinement seen in the Sez6 TKO cerebellum may well extend to these additional motor areas as we noted immature dendritic spine morphologies in the cortex.

This study provides evidence that Sez6 family protein expression is required for normal density and morphology of dendritic spines across multiple brain regions. A hallmark of many neurodevelopmental and psychiatric disorders is aberrant dendritic spine formation and refinement (Penzes et al. 2011). Spine head growth or shrinkage occurs along with changes in synaptic strength during learning (Lang et al. 2004; Matsuzaki et al. 2004; Zhou et al. 2004; Kopec et al. 2006) and thus different spine subtypes have been proposed to underlie learning as opposed to memory. Smaller, "thin" spines form weaker synapses but are more prone to potentiation, thus they are thought to underlie learning. "Mushroom" spines with larger heads, more AMPA receptors, and stronger synaptic responses exhibit long-term stability and are therefore thought to be responsible for memory (Matsuzaki et al. 2001; Holtmaat et al. 2005; Zuo et al. 2005). The Golgi-Cox analysis performed in this study revealed that

lack of Sez6 family proteins did not affect overall density of spines on somatosensory cortex layer V neurons but shifted spine morphology away from mushroom spines toward thin spines. This contrasts with results from Sez6 KO mice", which exhibited decreased spine density in the somatosensory cortex (Gunnersen et al. 2007; Zhu et al. 2016); however, in the current study, only basal rather than apical dendritic branches were scored for spines. In the hippocampus, Sez6 family proteins appear to regulate dendritic spine density as we observed a small but significant reduction in hippocampal spine density, consistent with results in Sez6 KO mice (Zhu et al. 2016), that appeared to be driven primarily by a decrease in mushroom spines. The role of Sez6 family proteins in regulating dendritic spine density may, in part, be mediated by the shed ectodomains of Sez6 family proteins as inhibition of shedding reduced spine density in the somatosensory cortex of WT mice to the same level as that seen in untreated Sez6 KO mice (Zhu et al. 2016). Thus, this study and others consistently report alterations to dendritic spines in mice lacking Sez6 family proteins.

The electrophysiological measurement of the intrinsic neuronal and synaptic properties of prefrontal pyramidal neurons revealed decreased membrane resistance and increased steady-state current at positive holding potentials, suggesting that Sez6 TKO neurons may have a greater density of potassium leak channels and voltage-gated potassium channels, respectively. Furthermore, Sez6 TKO neuron sEPSC amplitude was increased compared to WT, which may reflect altered network activity in Sez6 TKO mice. As Sez6 KO mice have previously been shown to have normal paired pulse facilitation (Gunnersen et al. 2007), the increased sEPSC amplitude is most likely a result of postsynaptic alterations. As such, this result raises the possibility that Sez6 TKO medial prefrontal cortex (mPFC) pyramidal neurons have a greater density and/or greater conductance of synaptic glutamate receptors. The immature spine morphologies seen in the somatosensory cortex would tend to indicate that the AMPA receptor levels at individual excitatory synapses are not increased, arguing in favor of enhanced conductance. Even so, dendritic spine properties may differ across brain regions (Ballesteros-Yáñez et al. 2006) so correlation of mPFC spine and electrophysiological properties would likely be informative. With the results presented here, it is tempting to speculate Sez6 family members may somehow regulate surface expression of GluA2, calcium impermeable AMPA subunits that, when incorporated, result in AMPA receptors with lower conductance than GluA1 homomeric AMPA receptors (Isaac et al. 2007). As such, Sez6 family proteins may promote the maturation and release of GluA2 subunits from the ER, where Sez6 family proteins are localized (Miyazaki et al. 2006), or may act to retain GluA2 containing AMPARs at the synapse. More in-depth electrophysiological and biochemical studies would be needed to fully understand how Sez6 family members influence synaptic function. However, the localization of Sez6 family members to the endoplasmic reticulum (Miyazaki et al. 2006) and role of Sez6 in promoting maturation and surface expression of GluK 2/3 (Pigoni et al., under review) suggests that Sez6 family members could be involved in regulating maturation and surface expression of other glutamate receptors also.

Coordinated synaptic activity across diverse brain regions is critical for generating appropriate behavioral responses to a stimulus. In forebrain regions crucial for learning and memory, such as the limbic system (e.g., *hippocampus*, amygdala) and neocortex, there is widespread expression of Sez6 and Sez6L proteins (Miyazaki et al. 2006; Gunnersen et al. 2007; Osaki et al. 2011; Pigoni et al. 2016), and we show here that the Sez6L2 protein is also strongly expressed in these regions. Sez6 exhibits an exclusively neuronal expression pattern in the healthy mouse brain, based on the morphologies and distributions of immunostained cells and the lack of Sez6 colocalization with the astrocytic marker GFAP (Kim 2005; Gunnersen et al. 2007). Although more extensive, the cellular distributions of Sez6L and Sez6L2 expression appear similar to that of Sez6; however, cell type-specific immunostaining would be needed to confirm that their expression is limited to neurons.

We found that Sez6 TKO mice had enhanced fear learning at 24 h post-training compared to WT mice. In contextual fear learning, initial learning about the context occurs in the hippocampus and then coordinated activity in the hippocampus, PFC, and amygdala allows association of the context with the aversive stimulus and fear expression (reviewed by Maren et al. 2013; Janak and Tye 2015). Inactivation of any of these brain regions can disrupt contextual fear memory (Muller et al. 1997; Zhu et al. 2014). For example, inactivation of the mPFC, specifically the prelimbic cortex, results in reduced fear expression (Corcoran and Quirk 2007), and conversely, stimulation of PrL cortical neurons that project to the amygdala promotes fear expression (Vidal-Gonzalez et al. 2006; Sierra-Mercado et al. 2011). While fear and anxiety-like states are provoked by different stimuli, with fear generally an adaptive response to imminent threats and anxiety related to potential threats, similar but distinct hippocampal-PFC-amygdala circuits underlie both of these responses (reviewed by Babaev et al. 2018). The possibility for a role of Sez6 family protein expression in the amygdala is also indicated by the enhanced stress responsiveness and anxiety-like phenotype of Sez6 TKO mice seen on the EOF and zero maze, opening up interesting future directions for investigating the precise sites of action of Sez6 family proteins. Together, these results suggest that the deletion of Sez6 family proteins leads to a heightened fear response following an aversive stimulus.

Dysregulation of hippocampal-PFC circuits in Sez6 TKO mice is further evidenced by working and short-term spatial memory deficits observed in these mice. Spatial working memory tasks, such as the spontaneous alternation Y maze utilized in this study, rely on interaction between the PFC and hippocampus (Yoon et al. 2008). Strong synchronous activity (theta-oscillation synchronicity) has been observed between the hippocampus and PFC during spatial working memory and suggests that the hippocampal to PFC pathway plays a role (Siapas et al. 2005; Sigurdsson et al. 2010; Mukai et al. 2015; Myroshnychenko et al. 2017). This pathway has been found to be crucial to many cognitive functions that rely on both the PFC and hippocampus with aberrant functional connectivity in this pathway linked to several neurodevelopmental disorders, such as schizophrenia in which working memory is commonly disrupted (Godsil et al. 2013; Li et al. 2015). The short-term memory deficit we observed in Sez6 TKO mice in the novel arm Y maze appears to be confined to hippocampal-dependent, spatial memory as performance on the NOR task, which tested novel object preference and is thought be primarily dependent on the perirhinal cortex (Wan et al. 2004; Barker and Warburton 2011; Olarte-Sánchez et al. 2015), was normal. These behavioral data are consistent with our observation that Sez6 TKO mice have a lower density of dendritic spines in the hippocampus and suggest that synaptic alterations in the hippocampus may be one mechanism underlying the deficits in working and short-term spatial memory.

Interestingly, we found that while lack of Sez6 family members resulted in a deficit in spatial working memory and short-term memory, long-term spatial memory remained intact. This may seem counterintuitive given the reduced hippocampal spine density observed in Sez6 TKO mice; however, intact hippocampal-dependent spatial learning accompanied by reduced spine density has been observed before in mice lacking Shank1 (Hung et al. 2008). The phenomenon of impaired working memory and short-term spatial memory but intact long-term memory has also been observed before, for example, in mice lacking the AMPA receptor subunit GluA1 (Reisel et al. 2002) and in mice lacking mGluR7 (Hölscher et al. 2004). GluA1 KO mice performed below chance level in the T-maze alternation task, similar to the Y maze alternation task used to test Sez6 TKO mice, and showed no preference for the novel arm in the novel arm Y maze but could adequately acquire the MWM task (Reisel et al. 2002; Schmitt et al. 2003; Sanderson et al. 2007, 2009). In GluA1 KO mice, the ability of a weaker stimulus to induce hippocampal short-term potentiation (STP) was greatly diminished when GluA1 was lacking (Erickson et al. 2010) while LTP was generally unaffected (Hoffman et al. 2002; Frey et al. 2009 but see Terashima et al. 2019) suggesting that GluA1 contributes more to the early component of LTP, believed to be a potential mechanism for working and short-term memory (Schulz and Fitzgibbons 1997; Fiebig and Lansner 2017). This phenotype in GluA1 KO mice was of particular interest given Sez6L2 has recently been found to bind GluA1 and link it to the cytoskeleton via adducin (Yaguchi et al. 2017). Nevertheless, more work is needed to determine whether STP or LTP is perturbed in Sez6 TKO mice although work with Sez6 KO mice indicates hippocampal LTP is impaired (Zhu et al. 2016). Together these data suggest that Sez6 family proteins are required for working and short-term spatial memory but that long-term memory may be formed and refined in a process that is not dependent upon Sez6 family proteins. It may be that, as the MWM makes use of multiple trials across several days to support memory formation, Sez6 TKO mice require repeated exposure to the task to sufficiently form the memory. Additionally, unlike the spontaneous and novel arm Y maze, which utilize a rodents' natural exploratory drive, the MWM and contextual fear conditioning make use of motivators, footshock, and water, which may act to enhance and/or support Sez6 TKO memory formation in these paradigms.

Further linking lack of Sez6 family proteins to hippocampal and PFC dysfunction is the observation that Sez6 TKO mice demonstrated cognitive inflexibility in the reversal portion of the MWM. Cognitive flexibility is the ability to rapidly change behavior in response to a change in circumstances, such as reversal learning, and requires the adjustment and updating of behavior to better reflect rules that have been changed (Armbruster et al. 2012; Dajani and Uddin 2015; Izquierdo et al. 2017). This executive function is often impaired in people with ASD (Lopez et al. 2005; Yerys et al. 2009) and schizophrenia (Murray et al. 2008; Leeson et al. 2009). Although spatial learning was intact for the acquisition phase of the MWM, Sez6 TKO mice demonstrated cognitive inflexibility with persistent searching in the old target quadrant during reversal and failure to adapt their search strategy. Impaired reversal learning in spatial memory tasks accompanied by intact acquisition has been observed in previously in mice with lesions of the mPFC (de Bruin et al. 1994; Lacroix et al. 2002; McDonald et al. 2008; Latif-Hernandez et al. 2016) and in mice with LTD deficits in the hippocampus and the mPFC (Nicholls et al. 2008; Dong et al. 2013; Mills et al. 2014; Ma et al. 2015) where the failure of the old memory to depotentiate is thought to interfere with storage and consolidation of the new memory. In addition to the PFC and hippocampus, the striatum, which forms reciprocal connections with the PFC, has been implicated in reversal learning because lesions of the striatum impair reversal learning in several paradigms (Ragozzino 2007; Castañé et al. 2010; Amodeo et al. 2017). These results support a role for the Sez6 family proteins in mediating flexible thinking; however, as Sez6 family proteins are so widely expressed throughout the brain, region-specific activation/inactivation studies will be needed to determine whether their expression in the hippocampus, PFC, or other region/s underlies their role in cognitive flexibility.

Neurodevelopmental disorders, such as ASD and schizophrenia, are associated with learning and memory deficits, cognitive inflexibility, social communication abnormalities and, in many cases, impaired motor ability (American Psychiatric Association 2013). These disorders, and others to which genetic variants in human homologs of Sez6 family proteins have been linked (Kumar et al. 2008; Konyukh et al. 2011; Xu et al. 2013; Cukier et al. 2014; Gilissen et al. 2014; Chapman et al. 2015; Mariani et al. 2015; Ambalavanan et al. 2016), have similar synaptic and behavioral features that likely reflect dysfunction in similar underlying circuits and pathways (Schubert et al. 2015; Gandal et al. 2018). Indeed dysregulation of genes involved in synaptic function and communication is a common feature with many genes implicated in multiple neurodevelopmental disorders (O'Dushlaine et al. 2011; De Rubeis et al. 2014; reviewed by Bourgeron 2015; Hall et al. 2015; Hormozdiari et al. 2015; Wang et al. 2018). The consistent effects of Sez6 family protein KO on synapse structure and function, described here and previously by us and others (Miyazaki et al. 2006; Gunnersen et al. 2007; Zhu et al. 2016), provide evidence that the regulation of dendritic spine structure and function likely underlies the behavioral deficits observed in Sez6 TKO mice. Although the exact mechanism/s by which Sez6 family proteins mediate these effects are still unclear, one possibility is activation of calcium signaling pathways. This is consistent with the lower level of protein kinase C activation seen in the Sez6 TKO cerebellum (Miyazaki et al. 2006) and blunted calcium signaling in cultured neurons upon knockdown of each of the Sez6 family proteins, individually (Anderson et al. 2012). Furthermore, Sez6 family proteins could be involved in regulating glutamate receptor maturation and trafficking, an idea supported by recent work demonstrating that Sez6L2 and GluA1 interact via their extracellular domains (Yaguchi et al. 2017), that Sez6 is involved in maturation of GluK 2/3 during trafficking to the neuron surface (Pigoni et al., under review), and that other CUB and/or SCR domain containing proteins in the CNS are important regulators of neurotransmitter receptor trafficking and function.

In addition to potential roles in neurodevelopmental disorders, Sez6 and Sez6L have been found to be two of the major substrates of the AD protease, BACE1 (Kuhn et al. 2012). A Sez6 variant has been associated with AD (Paracchini et al. 2018) and soluble Sez6 is reduced in the CSF of AD patients (Khoonsari et al. 2016). Treatment with BACE inhibitors reduces production of soluble Sez6 and Sez6L ectodomains (Pigoni et al. 2016) and negatively affects LTP and dendritic spine density in a Sez6-dependent manner (Zhu et al. 2016). The recent termination of a BACE inhibitor clinical trial for prodromal AD due to cognitive worsening (Egan et al. 2019) and the possible negative cognitive effects seen in a second trial (Henley et al. 2019) suggest that impaired processing of substrates other than amyloid

precursor protein, such as Sez6 family members, may be detrimental to cognitive functioning. The work presented here further supports such an interpretation by demonstrating that Sez6 family proteins act to support normal cognitive function and dendritic spine structure and function. Whether these functions are dependent on full-length or soluble Sez6 family proteins is not yet known.

In conclusion, our findings demonstrate that lack of Sez6 family proteins results in anxiety-like behavior, enhanced fear memory, working and short-term spatial memory deficits, cognitive inflexibility, and changes to dendritic spine density and morphology. The behavioral phenotypes found in the Sez6 TKO are, in many cases, similar to deficits seen in models of neurodevelopmental and psychiatric disorders. Therefore, these results contribute to the body of evidence that links Sez6 family proteins to the cognitive and motor deficits observed in patients with neurodevelopmental disorders, such as autism and schizophrenia.

Supplementary Material

Supplementary material is available at *Cerebral Cortex* online.

Funding

National Health and Medical Research Council (NHMRC) of Australia project (grant no. 1058672 to J.M.G.); NHMRC—Australian Research Council (ARC) Dementia Research Development Fellowship (K.M.M); Deutsche Forschungsgemeinschaft (German Research Foundation) within the framework of the Munich Cluster for Systems Neurology (EXC 2145 SyNergy to S.F.L.).

Notes

We wish to thank Ms Sarah Taverner, Ms Teresa Drever, and Ms Maya Kesar of the Biomedical Sciences Animal Facility, University of Melbourne, for the management and care of the WT and Sez6 TKO mouse lines; Dr Sue Finch of the Melbourne Statistical Consulting Platform, University of Melbourne, for her assistance with statistical analyses; Ms Yvette Wilson for her expert advice regarding contextual fear conditioning; and Ms Kathleen Teng for her technical help. *Conflict of Interest*: None declared.

References

Ambalavanan A, Girard S, Ahn K, Zhou S, Dionne-Laporte A, Spiegelman D, Bourassa C, Gauthier J, Hamdan F, Xiong L *et al*. 2016. De novo variants in sporadic cases of childhood onset schizophrenia. *Eur J Hum Genet*. 24:944–948.

American Psychiatric Association. 2013. *Diagnostic and statistical manual of mental disorders*. 5th ed. Arlington (VA): American Psychiatric Publishing.

Amodeo D, Rivera E, Cook E, Sweeney J, Ragozzino M. 2017. 5HT2A receptor blockade in dorsomedial striatum reduces repetitive behaviors in BTBR mice. *Genes Brain Behav*. 16:342–351.

Anderson G, Galfin T, Xu W, Aoto J, Malenka R, Südhof T. 2012. Candidate autism gene screen identifies critical role for cell-adhesion molecule CASPR2 in dendritic arborization and spine development. *Proc Natl Acad Sci U S A*. 109:18120–18125.

Armbruster D, Ueltzhoffer K, Basten U, Fiebach C. 2012. Prefrontal cortical mechanisms underlying individual differences in cognitive flexibility and stability. *J Cogn Neurosci*. 24:2385–2399.

Babaev O, Piletti Chatain C, Krueger-Burg D. 2018. Inhibition in the amygdala anxiety circuitry. *Exp Mol Med*. 50:18.

Ballesteros-Yáñez I, Benavides-Piccione R, Elston G, Yuste R, DeFelipe J. 2006. Density and morphology of dendritic spines in mouse neocortex. *Neuroscience*. 138:403–409.

Barbeau E, Meilleur A, Zeffiro T, Mottron L. 2015. Comparing motor skills in autism spectrum individuals with and without speech delay. *Autism Res*. 8:682–693.

Barker G, Warburton E. 2011. When is the hippocampus involved in recognition memory? *J Neurosci*. 31:10721–10731.

Boonen M, Staudt C, Gilis F, Oorschot V, Klumperman J, Jadot M. 2016. Cathepsin D and its newly identified transport receptor SEZ6L2 can modulate neurite outgrowth. *J Cell Sci*. 129:557–568.

Bork P, Beckmann G. 1993. The CUB domain. A widespread module in developmentally regulated proteins. *J Mol Biol*. 231:539–545.

Borsche M, Hahn S, Hanssen H, Munchau A, Wandinger K, Bruggemann N. 2019. Sez6L2-antibody-associated progressive cerebellar ataxia: a differential diagnosis of atypical parkinsonism. *J Neurol*. 266:522–524.

Bourgeron T. 2015. From the genetic architecture to synaptic plasticity in autism spectrum disorder. *Nat Rev Neurosci*. 16:551–563.

Brody D, Holtzman D. 2006. Morris water maze search strategy analysis in PDAPP mice before and after experimental traumatic brain injury. *Exp Neurol*. 197:330–340.

Castañé A, Theobald D, Robbins T. 2010. Selective lesions of the dorsomedial striatum impair serial spatial reversal learning in rats. *Behav Brain Res*. 210:74–83.

Chapman N, Nato A, Bernier R, Ankenman K, Sohi H, Munson J, Patowary A, Archer M, Blue E, Webb S *et al*. 2015. Whole exome sequencing in extended families with autism spectrum disorder implicates four candidate genes. *Hum Genet*. 134:1055–1068.

Chen C, Kano M, Abeliovich A, Chen L, Bao S, Kim J, Hashimoto K, Thompson R, Tonegawa S. 1995. Impaired motor coordination correlates with persistent multiple climbing fiber innervation in PKCγ mutant mice. *Cell*. 83:1233–1242.

Copits B, Robbins J, Frausto S, Swanson G. 2011. Synaptic targeting and functional modulation of GluK1 kainate receptors by the auxiliary neuropilin and tolloid-like (NETO) proteins. *J Neurosci*. 31:7334–7340.

Corcoran K, Quirk G. 2007. Activity in prelimbic cortex is necessary for the expression of learned, but not innate, fears. *J Neurosci*. 27:840–844.

Crépel F, Delhaye-Bouchaud N, Guastavino JM, Sampaio I. 1980. Multiple innervation of cerebellar Purkinje cells by climbing fibres in staggerer mutant mouse. *Nature*. 283:483–484.

Cukier H, Dueker N, Slifer S, Lee J, Whitehead P, Lalanne E, Leyva N, Konidari I, Gentry R, Hulme W *et al*. 2014. Exome sequencing of extended families with autism reveals genes shared across neurodevelopmental and neuropsychiatric disorders. *Mol Autism*. 5:1.

Dajani D, Uddin L. 2015. Demystifying cognitive flexibility: implications for clinical and developmental neuroscience. *Trends Neurosci*. 38:571–578.

Dang M, Yokoi F, Yin H, Lovinger D, Wang Y, Li Y. 2006. Disrupted motor learning and long-term synaptic plasticity in mice lacking NMDAR1 in the striatum. *Proc Natl Acad Sci U S A*. 103:15254–15259.

de Bruin J, Sanchez-Santed F, Heinsbroek R, Donker A, Postmes P. 1994. A behavioural analysis of rats with damage to the medial prefrontal cortex using the Morris water maze: evidence for behavioural flexibility, but not for impaired spatial navigation. *Brain Res*. 652:323–333.

De Rubeis S, He X, Goldberg A, Poultney C, Samocha K, Cicek A, Kou Y, Liu L, Fromer M, Walker S *et al*. 2014. Synaptic, transcriptional and chromatin genes disrupted in autism. *Nature*. 515:209–215.

Dong Z, Bai Y, Wu X, Li H, Gong B, Howland J, Huang Y, He W, Li T, Wang Y. 2013. Hippocampal long-term depression mediates spatial reversal learning in the Morris water maze. *Neuropharmacology*. 64:65–73.

Durieux P, Schiffmann S, de Kerchove d'Exaerde A. 2012. Differential regulation of motor control and response to dopaminergic drugs by D1R and D2R neurons in distinct dorsal striatum subregions. *EMBO J*. 31:640–653.

Egan M, Kost J, Voss T, Mukai Y, Aisen P, Cummings J, Tariot P, Vellas B, van Dyck C, Boada M *et al*. 2019. Randomized trial of verubecestat for prodromal Alzheimer's disease. *N Engl J Med*. 380:1408–1420.

Erickson M, Maramara L, Lisman J. 2010. A single brief burst induces GluR1-dependent associative short-term potentiation: a potential mechanism for short-term memory. *J Cogn Neurosci*. 22:2530–2540.

Fiebig F, Lansner A. 2017. A spiking working memory model based on Hebbian short-term potentiation. *J Neurosci*. 37:83–96.

Frey M, Sprengel R, Nevian T. 2009. Activity pattern-dependent long-term potentiation in neocortex and hippocampus of GluA1 (GluR-A) subunit-deficient mice. *J Neurosci*. 29:5587–5596.

Gandal M, Haney J, Parikshak N, Leppa V, Ramaswami G, Hartl C, Schork A, Appadurai V, Buil A, Werge T *et al*. 2018. Shared molecular neuropathology across major psychiatric disorders parallels polygenic overlap. *Science*. 359:693–697.

Gendrel M, Rapti G, Richmond J, Bessereau J. 2009. A secreted complement-control-related protein ensures acetylcholine receptor clustering. *Nature*. 461:992–996.

Gilissen C, Hehir-Kwa J, Thung D, van de Vorst M, van Bon B, Willemsen M, Kwint M, Janssen I, Hoischen A, Schenck A *et al*. 2014. Genome sequencing identifies major causes of severe intellectual disability. *Nature*. 511:344–347.

Godsil B, Kiss J, Spedding M, Jay T. 2013. The hippocampal-prefrontal pathway: the weak link in psychiatric disorders? *Eur Neuropsychopharmacol*. 23:1165–1181.

Gunnersen J, Kim M, Fuller S, De Silva M, Britto J, Hammond V, Davies P, Petrou S, Faber E, Sah P *et al*. 2007. Sez-6 proteins affect dendritic arborization patterns and excitability of cortical pyramidal neurons. *Neuron*. 56:621–639.

Hall J, Trent S, Thomas K, O'Donovan M, Owen M. 2015. Genetic risk for schizophrenia: convergence on synaptic pathways involved in plasticity. *Biol Psychiatry*. 77:52–58.

Henley D, Raghavan N, Sperling R, Aisen P, Raman R, Romano G. 2019. Preliminary results of a trial of Atabecestat in preclinical Alzheimer's disease. *N Engl J Med*. 380:1483–1485.

Herms J, Dorostkar M. 2016. Dendritic spine pathology in neurodegenerative diseases. *Annu Rev Pathol*. 11:221–250.

Hoffman D, Sprengel R, Sakmann B. 2002. Molecular dissection of hippocampal theta-burst pairing potentiation. *Proc Natl Acad Sci U S A*. 99:7740–7745.

Hölscher C, Schmid S, Pilz P, Sansig G, van der Putten H, Plappert C. 2004. Lack of the metabotropic glutamate receptor subtype 7 selectively impairs short-term working memory but not long-term memory. *Behav Brain Res*. 154:473–481.

Holtmaat A, Trachtenberg J, Wilbrecht L, Shepherd G, Zhang X, Knott G, Svoboda K. 2005. Transient and persistent dendritic spines in the neocortex in vivo. *Neuron*. 45:279–291.

Hormozdiari F, Penn O, Borenstein E, Eichler E. 2015. The discovery of integrated gene networks for autism and related disorders. *Genome Res*. 25:142–154.

Hung A, Futai K, Sala C, Valtschanoff J, Ryu J, Woodworth M, Kidd F, Sung C, Miyakawa T, Bear M *et al*. 2008. Smaller dendritic spines, weaker synaptic transmission, but enhanced spatial learning in mice lacking Shank1. *J Neurosci*. 28:1697–1708.

Isaac J, Ashby M, McBain C. 2007. The role of the GluR2 subunit in AMPA receptor function and synaptic plasticity. *Neuron*. 54:859–871.

Izquierdo A, Brigman J, Radke A, Rudebeck P, Holmes A. 2017. The neural basis of reversal learning: an updated perspective. *Neuroscience*. 345:12–26.

Janak P, Tye K. 2015. From circuits to behaviour in the amygdala. *Nature*. 517:284–292.

Kakizawa S, Yamasaki M, Watanabe M, Kano M. 2000. Critical period for activity-dependent synapse elimination in developing cerebellum. *J Neurosci*. 20:4954–4961.

Kano M, Hashimoto K, Kurihara H, Watanabe M, Inoue Y, Aiba A, Tonegawa S. 1997. Persistent multiple climbing fiber innervation of cerebellar Purkinje cells in mice lacking mGluR1. *Neuron*. 18:71–79.

Khoonsari P, Haggmark A, Lonnberg M, Mikus M, Kilander L, Lannfelt L, Bergquist J, Ingelsson M, Nilsson P, Kultima K *et al*. 2016. Analysis of the cerebrospinal fluid proteome in Alzheimer's disease. *PLoS One*. 11:e0150672.

Kiehn O. 2016. Decoding the organization of spinal circuits that control locomotion. *Nat Rev Neurosci*. 17:224–238.

Kim M. 2005. *Gene expression and gene function in the developing neocortex*. Doctoral diss: The University of Melbourne.

Konyukh M, Delorme R, Chaste P, Leblond C, Lemiere N, Nygren G, Anckarsater H, Rastam M, Stahlberg O, Amsellem F *et al*. 2011. Variations of the candidate SEZ6L2 gene on chromosome 16p11.2 in patients with autism spectrum disorders and in human populations. *PLoS One*. 6:e17289.

Kopec C, Li B, Wei W, Boehm J, Malinow R. 2006. Glutamate receptor exocytosis and spine enlargement during chemically induced long-term potentiation. *J Neurosci*. 26:2000–2009.

Kuhn P, Koroniak K, Hogl S, Colombo A, Zeitschel U, Willem M, Volbracht C, Schepers U, Imhof A, Hoffmeister A *et al*. 2012. Secretome protein enrichment identifies physiological BACE1 protease substrates in neurons. *EMBO J*. 31:3157–3168.

Kumar R, KaraMohamed S, Sudi J, Conrad D, Brune C, Badner J, Gilliam T, Nowak N, Cook E, Dobyns W *et al*. 2008. Recurrent 16p11.2 microdeletions in autism. *Hum Mol Genet*. 17: 628–638.

Lacroix L, White I, Feldon J. 2002. Effect of excitotoxic lesions of rat medial prefrontal cortex on spatial memory. *Behav Brain Res*. 133:69–81.

Lang C, Barco A, Zablow L, Kandel E, Siegelbaum S, Zakharenko S. 2004. Transient expansion of synaptically connected dendritic spines upon induction of hippocampal long-term potentiation. *Proc Natl Acad Sci U S A*. 101:16665–16670.

Latif-Hernandez A, Shah D, Ahmed T, Lo A, Callaerts-Vegh Z, Van der Linden A, Balschun D, D'Hooge R. 2016. Quinolinic acid injection in mouse medial prefrontal cortex affects reversal learning abilities, cortical connectivity and hippocampal synaptic plasticity. *Sci Rep*. 6:36489.

Leeson V, Robbins T, Matheson E, Hutton S, Ron M, Barnes T, Joyce E. 2009. Discrimination learning, reversal, and set-shifting in first-episode schizophrenia: stability over six years and specific associations with medication type and disorganization syndrome. *Biol Psychiatry*. 66:586–593.

Lein E, Hawrylycz M, Ao N, Ayres M, Bensinger A, Bernard A, Boe A, Boguski M, Brockway K, Byrnes E *et al*. 2007. Genome-wide atlas of gene expression in the adult mouse brain. *Nature*. 445:168–176.

Li M, Long C, Yang L. 2015. Hippocampal-prefrontal circuit and disrupted functional connectivity in psychiatric and neurodegenerative disorders. *Biomed Res Int*. 2015:810548.

Lopez B, Lincoln A, Ozonoff S, Lai Z. 2005. Examining the relationship between executive functions and restricted, repetitive symptoms of autistic disorder. *J Autism Dev Disord*. 35:445–460.

Ma J, Duan Y, Qin Z, Wang J, Liu W, Xu M, Zhou S, Cao X. 2015. Overexpression of alphaCaMKII impairs behavioral flexibility and NMDAR-dependent long-term depression in the medial prefrontal cortex. *Neuroscience*. 310:528–540.

Maccarrone G, Ditzen C, Yassouridis A, Rewerts C, Uhr M, Uhlen M, Holsboer F, Turck C. 2013. Psychiatric patient stratification using biosignatures based on cerebrospinal fluid protein expression clusters. *J Psychiatr Res*. 47:1572–1580.

Maren S, Phan K, Liberzon I. 2013. The contextual brain: implications for fear conditioning, extinction and psychopathology. *Nat Rev Neurosci*. 14:417–428.

Mariani J, Coppola G, Zhang P, Abyzov A, Provini L, Tomasini L, Amenduni M, Szekely A, Palejev D, Wilson M *et al*. 2015. FOXG1-dependent dysregulation of GABA/glutamate neuron differentiation in autism spectrum disorders. *Cell*. 162:375–390.

Matsuzaki M, Ellis-Davies G, Nemoto T, Miyashita Y, Iino M, Kasai H. 2001. Dendritic spine geometry is critical for AMPA receptor expression in hippocampal CA1 pyramidal neurons. *Nat Neurosci*. 4:1086–1092.

Matsuzaki M, Honkura N, Ellis-Davies G, Kasai H. 2004. Structural basis of long-term potentiation in single dendritic spines. *Nature*. 429:761–766.

McDonald R, King A, Foong N, Rizos Z, Hong N. 2008. Neurotoxic lesions of the medial prefrontal cortex or medial striatum impair multiple-location place learning in the water task: evidence for neural structures with complementary roles in behavioural flexibility. *Exp Brain Res*. 187:419–427.

Miedel C, Patton J, Miedel A, Miedel E, Levenson J. 2017. Assessment of spontaneous alternation, novel object recognition and limb clasping in transgenic mouse models of amyloid-beta and tau neuropathology. *J Vis Exp*. 123:e55523.

Mills F, Bartlett T, Dissing-Olesen L, Wisniewska M, Kuznicki J, Macvicar B, Wang Y, Bamji S. 2014. Cognitive flexibility and long-term depression (LTD) are impaired following beta-catenin stabilization in vivo. *Proc Natl Acad Sci U S A*. 111:8631–8636.

Miyazaki T, Hashimoto K, Uda A, Sakagami H, Nakamura Y, Saito S, Nishi M, Kume H, Tohgo A, Kaneko I *et al*. 2006. Disturbance of cerebellar synaptic maturation in mutant mice lacking BSRPs, a novel brain-specific receptor-like protein family. *FEBS Lett*. 580:4057–4064.

Morley B, Campbell R. 1984. Internal homologies of the Ba fragment from human complement component factor B, a class III MHC antigen. *EMBO J*. 3:153–157.

Mukai J, Tamura M, Fenelon K, Rosen A, Spellman T, Kang R, MacDermott A, Karayiorgou M, Gordon J, Gogos J. 2015. Molecular substrates of altered axonal growth and brain connectivity in a mouse model of schizophrenia. *Neuron*. 86:680–695.

Muller J, Corodimas K, Fridel Z, LeDoux J. 1997. Functional inactivation of the lateral and basal nuclei of the amygdala by muscimol infusion prevents fear conditioning to an explicit conditioned stimulus and to contextual stimuli. *Behav Neurosci*. 111:683–691.

Murphy M, Newman R, Kita M, Wilson Y, Lopaticki S, Morahan G. 2004. Genetic analysis of stress responsiveness in a mouse model. *Aust J Psychol*. 56:108–114.

Murray G, Cheng F, Clark L, Barnett J, Blackwell A, Fletcher P, Robbins T, Bullmore E, Jones P. 2008. Reinforcement and reversal learning in first-episode psychosis. *Schizophr Bull*. 34:848–855.

Myroshnychenko M, Seamans J, Phillips A, Lapish C. 2017. Temporal dynamics of hippocampal and medial prefrontal cortex interactions during the delay period of a working memory-guided foraging task. *Cereb Cortex*. 27:5331–5342.

Ng D, Pitcher G, Szilard R, Sertie A, Kanisek M, Clapcote S, Lipina T, Kalia L, Joo D, McKerlie C *et al*. 2009. Neto1 is a novel CUB-domain NMDA receptor-interacting protein required for synaptic plasticity and learning. *PLoS Biol*. 7:e41.

Nicholls R, Alarcon J, Malleret G, Carroll R, Grody M, Vronskaya S, Kandel E. 2008. Transgenic mice lacking NMDAR-dependent LTD exhibit deficits in behavioral flexibility. *Neuron*. 58:104–117.

Nurnberger J, Koller D, Jung J, Edenberg H, Foroud T, Guella I, Vawter M, Kelsoe J, Psychiatric Genomics Consortium Bipolar G. 2014. Identification of pathways for bipolar disorder: a meta-analysis. *JAMA Psychiatry*. 71:657–664.

O'Dushlaine C, Kenny E, Heron E, Donohoe G, Gill M, Morris D, International Schizophrenia C, Corvin A. 2011. Molecular pathways involved in neuronal cell adhesion and membrane scaffolding contribute to schizophrenia and bipolar disorder susceptibility. *Mol Psychiatry*. 16:286–292.

Olarte-Sánchez C, Amin E, Warburton E, Aggleton J. 2015. Perirhinal cortex lesions impair tests of object recognition memory but spare novelty detection. *Eur J Neurosci*. 42:3117–3127.

Osaki G, Mitsui S, Yuri K. 2011. The distribution of the seizure-related gene 6 (Sez-6) protein during postnatal development of the mouse forebrain suggests multiple functions for this protein: an analysis using a new antibody. *Brain Res*. 1386:58–69.

Pandey K. 2009. Functional roles of short sequence motifs in the endocytosis of membrane receptors. *Front Biosci (Landmark Ed)*. 14:5339–5360.

Paquet A, Olliac B, Golse B, Vaivre-Douret L. 2016. Current knowledge on motor disorders in children with autism spectrum disorder (ASD). *Child Neuropsychol*. 22:763–794.

Paracchini L, Beltrame L, Boeri L, Fusco F, Caffarra P, Marchini S, Albani D, Forloni G. 2018. Exome sequencing in an Italian family with Alzheimer's disease points to a role for seizure-related gene 6 (SEZ6) rare variant R615H. *Alzheimers Res Ther*. 10:106.

Penzes P, Cahill M, Jones K, Van Leeuwen J, Woolfrey K. 2011. Dendritic spine pathology in neuropsychiatric disorders. *Nat Neurosci*. 14:285–293.

Pigoni M, Wanngren J, Kuhn P, Munro K, Gunnersen J, Takeshima H, Feederle R, Voytyuk I, De Strooper B, Levasseur M *et al*. 2016. Seizure protein 6 and its homolog seizure 6-like protein are physiological substrates of BACE1 in neurons. *Mol Neurodegener*. 11:67.

Piochon C, Kloth A, Grasselli G, Titley H, Nakayama H, Hashimoto K, Wan V, Simmons D, Eissa T, Nakatani J *et al*. 2014. Cerebellar plasticity and motor learning deficits in a copy-number variation mouse model of autism. *Nat Commun*. 5:5586.

Ragozzino M. 2007. The contribution of the medial prefrontal cortex, orbitofrontal cortex, and dorsomedial striatum to behavioral flexibility. *Ann N Y Acad Sci*. 1121:355–375.

Reisel D, Bannerman D, Schmitt W, Deacon R, Flint J, Borchardt T, Seeburg P, Rawlins J. 2002. Spatial memory dissociations in mice lacking GluR1. *Nat Neurosci*. 5:868–873.

Risher W, Patel S, Kim I, Uezu A, Bhagat S, Wilton D, Pilaz L, Singh Alvarado J, Calhan O, Silver D *et al*. 2014. Astrocytes refine cortical connectivity at dendritic spines. *eLife*. 3.

Rogers J, Churilov L, Hannan A, Renoir T. 2017. Search strategy selection in the Morris water maze indicates allocentric map formation during learning that underpins spatial memory formation. *Neurobiol Learn Mem*. 139:37–49.

Roitman M, Edgington-Mitchell L, Mangum J, Ziogas J, Adamides A, Myles P, Choo-Bunnett H, Bunnett N, Gunnersen J. 2019. Sez6 levels are elevated in cerebrospinal fluid of patients with inflammatory pain-associated conditions. *Pain Rep*. 4:e719.

Sanderson D, Good M, Skelton K, Sprengel R, Seeburg P, Rawlins J, Bannerman D. 2009. Enhanced long-term and impaired short-term spatial memory in GluA1 AMPA receptor subunit knockout mice: evidence for a dual-process memory model. *Learn Mem*. 16:379–386.

Sanderson D, Gray A, Simon A, Taylor A, Deacon R, Seeburg P, Sprengel R, Good M, Rawlins J, Bannerman D. 2007. Deletion of glutamate receptor-a (GluR-A) AMPA receptor subunits impairs one-trial spatial memory. *Behav Neurosci*. 121:559–569.

Schmitt W, Deacon R, Seeburg P, Rawlins J, Bannerman D. 2003. A within-subjects, within-task demonstration of intact spatial reference memory and impaired spatial working memory in glutamate receptor-A-deficient mice. *J Neurosci*. 23:3953–3958.

Schubert D, Martens G, Kolk S. 2015. Molecular underpinnings of prefrontal cortex development in rodents provide insights into the etiology of neurodevelopmental disorders. *Mol Psychiatry*. 20:795–809.

Schulz P, Fitzgibbons J. 1997. Differing mechanisms of expression for short- and long-term potentiation. *J Neurophysiol*. 78:321–334.

Shimizu-Nishikawa K, Kajiwara K, Kimura M, Katsuki M, Sugaya E. 1995. Cloning and expression of SEZ-6, a brain-specific and seizure-related cDNA. *Brain Res Mol Brain Res*. 28: 201–210.

Sia G, Clem R, Huganir R. 2013. The human language-associated gene SRPX2 regulates synapse formation and vocalization in mice. *Science*. 342:987–991.

Siapas A, Lubenov E, Wilson M. 2005. Prefrontal phase locking to hippocampal theta oscillations. *Neuron*. 46:141–151.

Sierra-Mercado D, Padilla-Coreano N, Quirk G. 2011. Dissociable roles of prelimbic and infralimbic cortices, ventral hippocampus, and basolateral amygdala in the expression and extinction of conditioned fear. *Neuropsychopharmacology*. 36:529–538.

Sigurdsson T, Stark K, Karayiorgou M, Gogos J, Gordon J. 2010. Impaired hippocampal-prefrontal synchrony in a genetic mouse model of schizophrenia. *Nature*. 464:763–767.

Steen V, Nepal C, Ersland K, Holdhus R, Naevdal M, Ratvik S, Skrede S, Havik B. 2013. Neuropsychological deficits in mice depleted of the schizophrenia susceptibility gene CSMD1. *PLoS One*. 8:e79501.

Terashima A, Suh Y, Isaac J. 2019. The AMPA receptor subunit GluA1 is required for CA1 hippocampal Long-term potentiation but is not essential for synaptic transmission. *Neurochem Res*. 44:549–561.

Vidal-Gonzalez I, Vidal-Gonzalez B, Rauch S, Quirk G. 2006. Microstimulation reveals opposing influences of prelimbic and infralimbic cortex on the expression of conditioned fear. *Learn Mem*. 13:728–733.

Wan H, Warburton E, Zhu X, Koder T, Park Y, Aggleton J, Cho K, Bashir Z, Brown M. 2004. Benzodiazepine impairment of perirhinal cortical plasticity and recognition memory. *Eur J Neurosci*. 20:2214–2224.

Wang R, Mellem J, Jensen M, Brockie P, Walker C, Hoerndli F, Hauth L, Madsen D, Maricq A. 2012. The SOL-2/Neto auxiliary protein modulates the function of AMPA-subtype ionotropic glutamate receptors. *Neuron*. 75:838–850.

Wang X, Christian K, Song H, Ming G. 2018. Synaptic dysfunction in complex psychiatric disorders: from genetics to mechanisms. *Genome Med*. 10:9.

Weiss L, Shen Y, Korn J, Arking D, Miller D, Fossdal R, Saemundsen E, Stefansson H, Ferreira M, Green T *et al*. 2008. Association between microdeletion and microduplication at 16p11.2 and autism. *N Engl J Med*. 358:667–675.

Xu C, Mullersman J, Wang L, Bin Su B, Mao C, Posada Y, Camarillo C, Mao Y, Escamilla M, Wang K. 2013. Polymorphisms in seizure 6-like gene are associated with bipolar disorder I: evidence of gene x gender interaction. *J Affect Disord*. 145:95–99.

Yaguchi H, Yabe I, Takahashi H, Okumura F, Takeuchi A, Horiuchi K, Kano T, Kanda A, Saito W, Matsumoto M *et al*. 2014. Identification of anti-Sez6l2 antibody in a patient with cerebellar ataxia and retinopathy. *J Neurol*. 261:224–226.

Yaguchi H, Yabe I, Takahashi H, Watanabe M, Nomura T, Kano T, Matsumoto M, Nakayama K, Watanabe M, Hatakeyama S. 2017. Sez6L2 regulates phosphorylation of ADD and neuritogenesis. *Biochem Biophys Res Commun*. 494:234–241.

Yerys B, Wallace G, Harrison B, Celano M, Giedd J, Kenworthy L. 2009. Set-shifting in children with autism spectrum disorders: reversal shifting deficits on the intradimensional/extradimensional shift test correlate with repetitive behaviors. *Autism*. 13:523–538.

Yin H, Mulcare S, Hilario M, Clouse E, Holloway T, Davis M, Hansson A, Lovinger D, Costa R. 2009. Dynamic reorganization of striatal circuits during the acquisition and consolidation of a skill. *Nat Neurosci*. 12:333–341.

Yoon T, Okada J, Jung M, Kim J. 2008. Prefrontal cortex and hippocampus subserve different components of working memory in rats. *Learn Mem*. 15:97–105.

Zhang W, St-Gelais F, Grabner C, Trinidad J, Sumioka A, Morimoto-Tomita M, Kim K, Straub C, Burlingame A, Howe J *et al*. 2009. A transmembrane accessory subunit that modulates kainate-type glutamate receptors. *Neuron*. 61:385–396.

Zheng Y, Mellem J, Brockie P, Madsen D, Maricq A. 2004. SOL-1 is a CUB-domain protein required for GLR-1 glutamate receptor function in *C. elegans*. *Nature*. 427:451–457.

Zhou Q, Homma K, Poo M. 2004. Shrinkage of dendritic spines associated with long-term depression of hippocampal synapses. *Neuron*. 44:749–757.

Zhu H, Pleil K, Urban D, Moy S, Kash T, Roth B. 2014. Chemogenetic inactivation of ventral hippocampal glutamatergic neurons disrupts consolidation of contextual fear memory. *Neuropsychopharmacology*. 39:1880–1892.

Zhu K, Xiang X, Filser S, Marinkovic P, Dorostkar M, Crux S, Neumann U, Shimshek D, Rammes G, Haass C *et al.* 2016. Beta-site amyloid precursor protein cleaving enzyme 1 inhibition impairs synaptic plasticity via seizure protein 6. *Biol Psychiatry*. 83:428–437.

Zuo Y, Lin A, Chang P, Gan W. 2005. Development of long-term dendritic spine stability in diverse regions of cerebral cortex. *Neuron*. 46:181–189.

© 2008 Allen Institute for Brain Science. Allen Mouse Brain Atlas. http://mousespinal.brain-map.org/.